AD NUMBER

AD481755

LIMITATION CHANGES

TO:

Approved for public release; distribution is unlimited.

FROM:

**Distribution authorized to U.S. Gov't. agencies and their contractors;
Administrative/Operational Use; 1962. Other requests shall be referred to U.S. Naval Postgraduate School, Monterey, CA 93943.**

AUTHORITY

USNPS ltr, 23 Sep 1971

A FRICTION AND WEAR STUDY OF CARBON IN SLIDING CONTACT WITH METAL

ROGER B. HORNE, JR.

A FRICTION AND WEAR STUDY OF CARBON IN SLIDING CONTACT WITH METAL

* * * * *

Roger B. Horne, Jr.

A FRICTION AND WEAR STUDY OF CARBON IN SLIDING CONTACT WITH METAL

by

Roger B. Horne, Jr.
//
Lieutenant, United States Navy

Submitted in partial fulfillment of
the requirements for the degree of

MASTER OF SCIENCE
IN
MECHANICAL ENGINEERING

United States Naval Postgraduate School

1 9 6 2

A FRICTION AND WEAR STUDY OF CARBON IN SLIDING CONTACT WITH METAL

by

Roger B. Horne, Jr.

This work is accepted as fulfilling
the thesis requirements for the degree of
MASTER OF SCIENCE
IN
MECHANICAL ENGINEERING
from the
United States Naval Postgraduate School

ABSTRACT

This investigation concerns the mechanical wear of carbon in sliding contact with metal. The combinations of carbon and metal materials tested were some of those normally used for mechanical seal applications. The investigation was carried out in two phases:

Material selction. Various combinations of carbon and metal were tested to determine which performed best on the basis of wear rate and friction.

Testing. The selected combination of materials was further tested to determine the predominant test parameters affecting wear rate and friction.

It was found that carbon wear rate is more dependent on contact pressure than applied load. It was also found that wear rate and friction increase with decreasing speed. This, along with other evidence, indicates that the establishment of a boundary film was of importance in this investigation.

A cross cylinder testing apparatus built at the United States Naval Postgraduate School was used for testing.

PREFACE

The wear characteristics of carbon, as is true with most materials, have not been studied extensively. Wear and friction theories are currently being developed; however, there are so many variables involved in mechanical wear, and they are so complexly related that it seems impossible to isolate causes and effects for analysis. It is believed that only through extensive investigations, will sufficient data and experience be accumulated to deal with what one author has so aptly called "....the tremendous trifle."

Professor Ernest K. Gatecombe, of the Naval Postgraduate School, Department of Mechanical Engineering, did much to promote this investigation with his inspiration and ingenuity. The author deeply thanks the United States Naval Engineering Experiment Station at Annapolis, Maryland and Messrs. W. V. Smith, M. R. Gross, and W. A. Tewes, Jr., at the Station, for their cooperation and suggestions throughout the project. The machine shop and Ken Mothersell did an excellent job of fabricating a testing apparatus which required many precision parts.

TABLE OF CONTENTS

LIST OF TABLES AND ILLUSTRATIONS

1. Introduction

Mechanical wear is defined as the harmful deterioration of a surface while in use; it is the major cause of costly repairs and reduced efficiency of machinery. Although the effects of friction and wear have been recognized for hundreds of years, there is no single empirical relationship that predicts wear. Investigators have in recent years accumulated some knowledge of the friction-wear phenomena, and now theories are being evolved.

In the fifteenth Centruy, Leonardo da Vinci did experiments that indicated his awareness of the Laws of Friction.[1] In 1699, these results were verified by Amentons, a French engineer, and have since been called "Amentons'Laws".[2] These laws are: friction force is independent of the area of contact between surfaces, and friction force is proportional to the load between surfaces. Later, in 1781, Coulomb distinguished between static and kinetic friction, giving attention to the possibility that molecular adhesion between the surfaces might be the cause of friction.[3] Today, the idea of molecular adhesion is the basis of most friction and wear theories.

Bowden and Tabor have shown that the real area of contact between surfaces is a small fraction of the apparent area of contact.[4] Figure 1 shows how the microscopic surface irregularities meet, keeping the larger part of the surface area from coming into contact. The contact area may be 1/100 to 1/10,000 of the apparent area.[5]

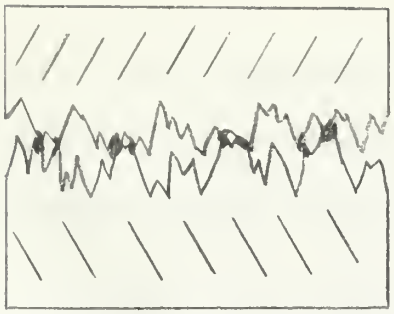

FIGURE 1

Equation (1) has been presented by Holm,[6] Burwell and Strang,[7] and Archard.[8] This equation predicts that

$$W = KL/P \qquad (1)$$

Where:

W = Volume loss per unit sliding distance

L = Normal load

P = Material flow pressure

K = Dimensionless constant

wear rate is independent of the apparent contact pressure between surfaces, and varies directly with normal load. The equation, which has been used to evaluate data from metal to metal and non-metal to non-metal wear tests, follows from the adhesion theory of friction, and is consistent with "Amentons' Laws."

Recently, Dorinson and Broman have maintained that wear rate is dependent on apparent contact pressure and not normal load.[9] They believe that the data obtained in varifying equation (1) has been misinterrepted, and used a new testing procedure, with metal specimens, to provide experimental evidence.

The concern of this investigation is the friction and wear characteristics of carbon under conditions experienced in seal applications. Tests were carried out on a cross cylinder testing apparatus which was instrumented to provide a continuous recording of the wear scar depth and frictional force.

Experimentation was carried out in two phases:

1. Several grades of carbon and different metal counterfaces were tested in all combinations to determine which pair of materials had the best friction and wear characteristics.

2. The selected materials were further tested to determine the effects on friction and wear as controllable test parameters were varied.

The data obtained is presented in a graphic display where possible. The actual reduced data is in tabular form in Appendix II. Photographs of equipment, traces recorded, and wear scars are included.

2. Description of Apparatus

The apparatus used in this investigation to test the wear characteristics of cylindrical specimens is such that the cylinders are in contact with their axes of revolution perpendicular to each other, and is thus called a cross cylinder testing apparatus. The cross cylinder testing apparatus was chosen so that results might be compared with testing being conducted out at the Naval Engineering Experiment Station (NEES) at Annapolis, Maryland. The cross cylinder test affords the possibility of making several runs on each specimen by a simple indexing. This, of course, leads to: less variation in results due to changing specimens, less expense in specimen preparation, and less time required in the testing procedure. The cross cylinder test has other advantages; for instance, it can be set up in the bed of a lathe or milling machine.[10] However, such a lathe or milling machine was not used in this investigation due to the speed limitations. Figures 2 through 5 show the apparatus fabricated at the United States Naval Postgraduate School for this study. Basic ideas were taken from the apparatus used at NEES Annapolis, Maryland.

The cross cylinder apparatus consists of a spindle A mounted in precision bearings on micrometer bench B[1]. The spindle is driven via a V-belt by a Vickers 3/4 horsepower hydraulic transmission C. The transmission is powered by a 1/2 horsepower, 115 volt, motor rated at 1725 RPM. The transmission and spindle pulleys have a 2:1 ratio respectively, thus

---

[1]Designation letters refer to figures 2 through 5

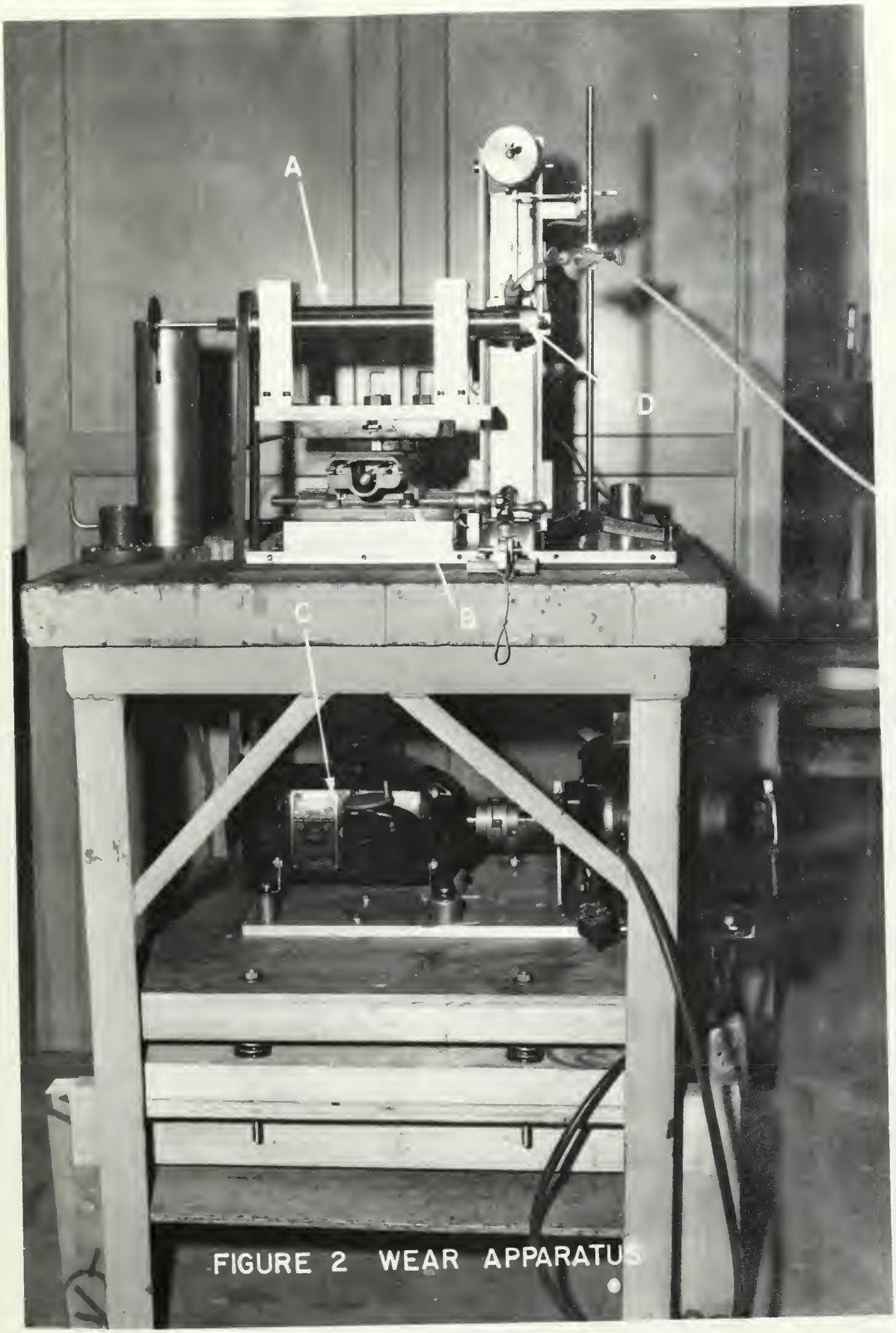

FIGURE 2 WEAR APPARATUS

making possible speeds of from 0 to 3450 RPM. The metal specimen D is rotated by the spindle, and can be indexed to any desired position with the micrometer bench. The carbon specimen E does not rotate, but is attached to the head F. This head, made of micarta, is free to rotate in a vertical plane as shown by a comparison of figures 3 and 4. The head is held in a horizontal position by wire G which is attached to a beam H by means of a yoke. The beam is removable, but is attached rigidly to the frame of the apparatus by a clamping device I. Details of the beam are given in figure 6. Four type A-5, SRA strain gages are mounted on the beam in a four gage bridge circuit, in order that beam strain caused by the frictional force between the surfaces can be measured. The load is transmitted from the load pan J to the carbon specimens by lever arms K. These lever arms pivot about bearing L. A linear variable differential transformer (LVDT) is mounted in the micarta block at the base of lever K. The core of the transformer is attached to micrometer N. As the carbon specimen is worn there is relative motion between the core and transformer, producing a signal proportional to the displacement. O is a brass counter-weight for initial balancing.

Lubrication is applied to the specimens by means of a small sponge that is fed distilled water that siphons through a plastic tube. Two valves are used to control the flow: a needle valve maintained at a constant opening to serve as a metering device, and a petcock to provide on-off control. The water is caught in a plastic container and filtered through spun glass for re-use.

The apparatus, with the exception of the micrometer bench and steel spindle, is made of non-magnetic materials to reduce distortion of the transformer field. The platform on which the motor and transmission

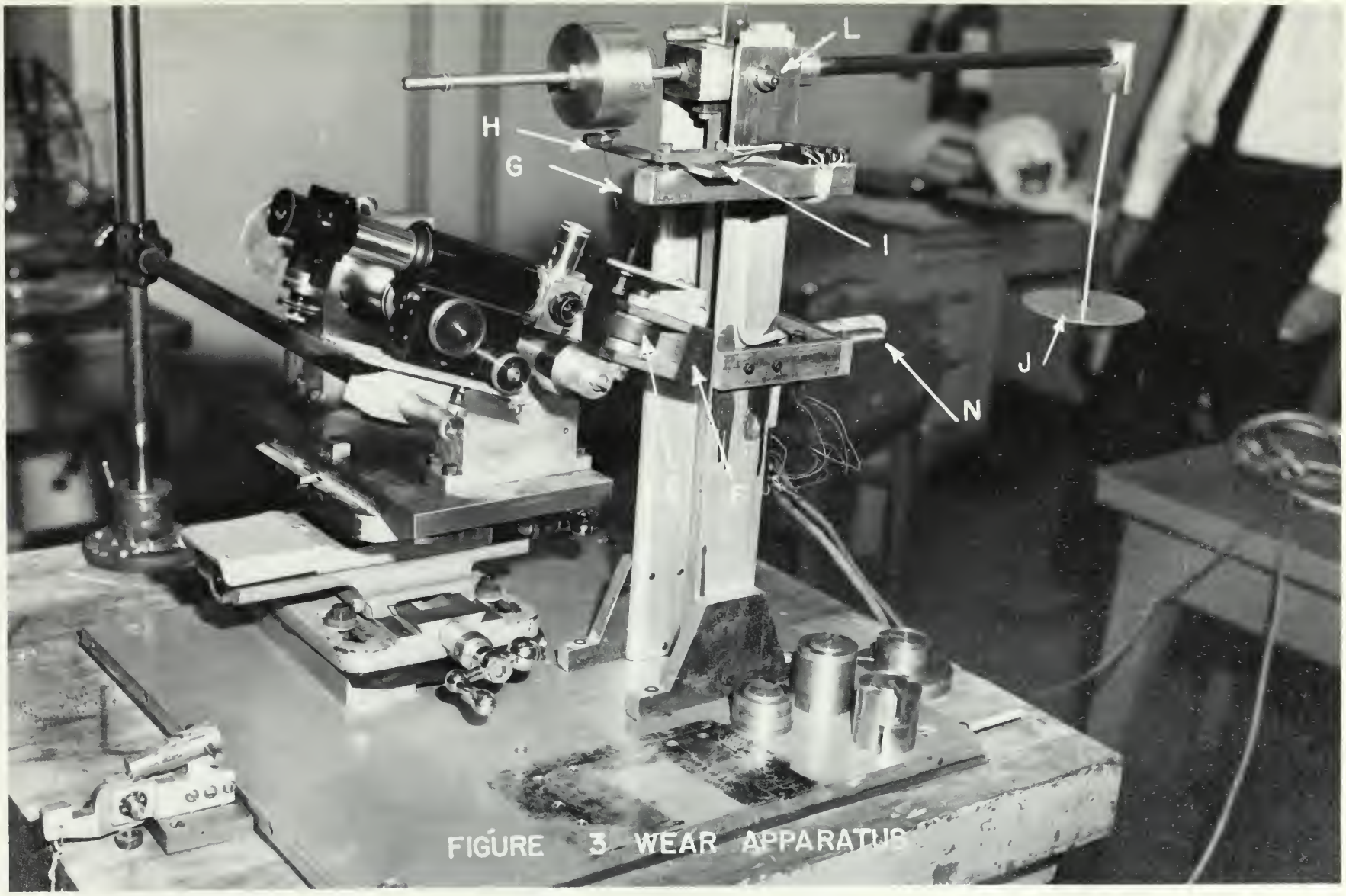

FIGURE 3 WEAR APPARATUS

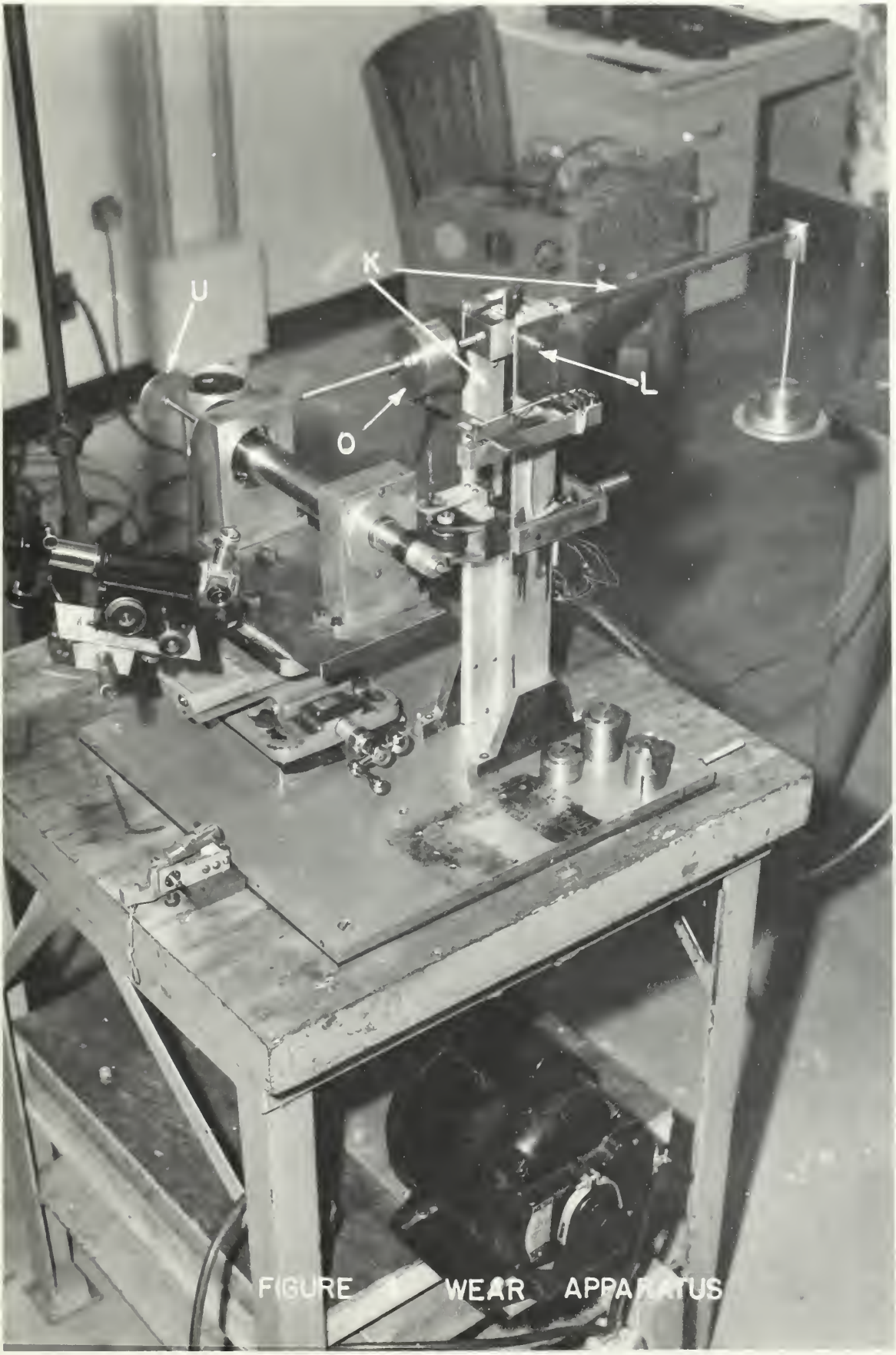

FIGURE WEAR APPARATUS

were mounted was supported by springs in order to reduce vibration and to maintain belt tension. The entire unit is used in a temperature controlled room with a heavy concrete floor.

3. Instrumentation

The apparatus is instrumented to record continuously wear scar depth and frictional force for constant-load runs. The author had previously instrumented the testing apparatus at NEES, Annapolis, Maryland to record wear depth. The same method was employed in this study with an apparatus especially designed to accommodate the instrumentation.

An Atcotran type 6204 Linear Variable Differential Transformer (LVDT) is used with a model 300BF Daytronic Differential Transformer Indicator P (DDI) to measure wear scar depth. The DDI has an output impedance of 50,000 ohms, a flat frequency response from 0 to 400 cps, and is accurate to 1% of the scale in use. There are five scale ranges available; when used with a matching transformer .100 in. to .001 in. core displacements give full scale deflections of the DDI meter. The DDI supplies the primary voltage of the transformer, and receives, amplifies, and rectifies the secondary voltage signal. The signal is recorded on a model 25 Moseley Autograph X-Y Recorder Q. This recorder responds with full scale deflection for sensitivities of 500 volts to 5 millivolts. The Y axis is employed to indicate the depth of wear; the X axis is the time axis. For most test runs the DDI was set at the .001 in. range and the X-Y recorder at the 50 mv range. With these settings, core displacements of .001 in. give full scale pen deflections.

Four type A-5, SR4 strain gages arranged in a bridge circuit, figure 6, are used to measure the frictional force transmitted to the beam. Power is supplied to the bridge by a model 130-2C Honeywell Heiland Carrier Amplifier System R. The system has an output impedance of 12 ohms, a

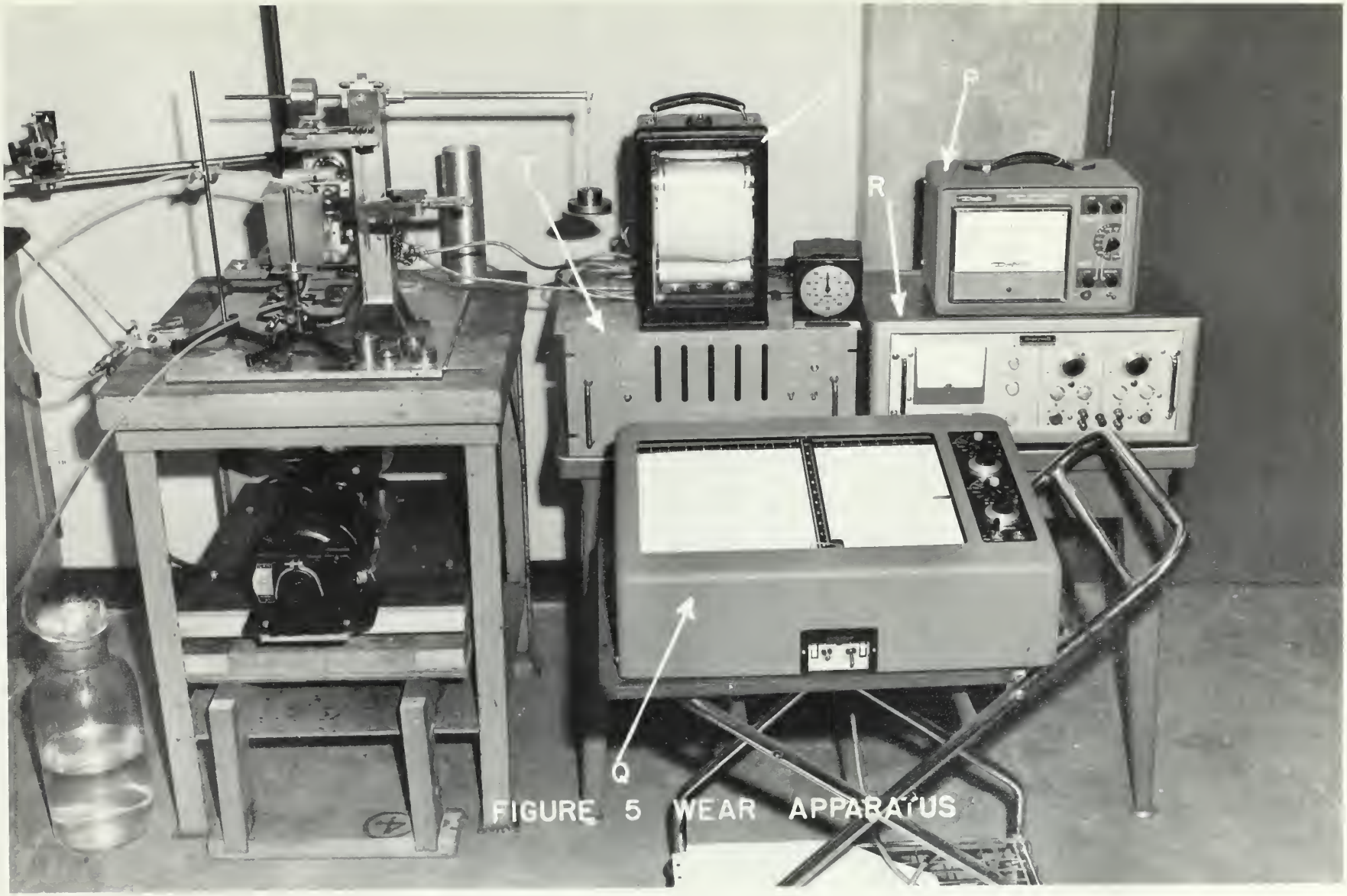

FIGURE 5 WEAR APPARATUS

frequency range of from 0 to 1000 cps, and is rated at $\pm$ 40 milliamps for a 25 ohm load. The output signal is sent to a model A. W., Esterling Angus Graphic Ammeter S. With this arrangement a 0.1 pound frictional force moves the recorder pen 1/5 full scale deflection.

A model 554S Berkeley E PUT meter T is used to count the number of spindle revolutions per second. This is accomplished by mounting a notched metal disc U on the spindle so that it rotates in a magnetic field produced by a magnet wrapped with 34 gage wire. The interruption of the field generates a measureable pulse voltage in the wire. The number of pulses per second corresponds to revolutions per second and are counted on the E PUT meter. This arrangement provides a very accurate and rapid means of checking the speed and adjusting it as desired.

A Bausch & Lomb microscope, with a micrometer eyepiece, is mounted such that it can be swung into a position to measure wear scar diameters without removing the specimens. The micrometer eyepiece has a movable scale 5 mm in length, and is divided into 1/5 mm divisions. There is a graduated drum divided into 100 divisions that moves the scale 1/5 mm for each revolution.

A type BL 103 Brush Surface Analyzer System figure 7, was used to measure the specimen surface roughnesses. Figures 11 through 16 illustrate the traces produced by this system.

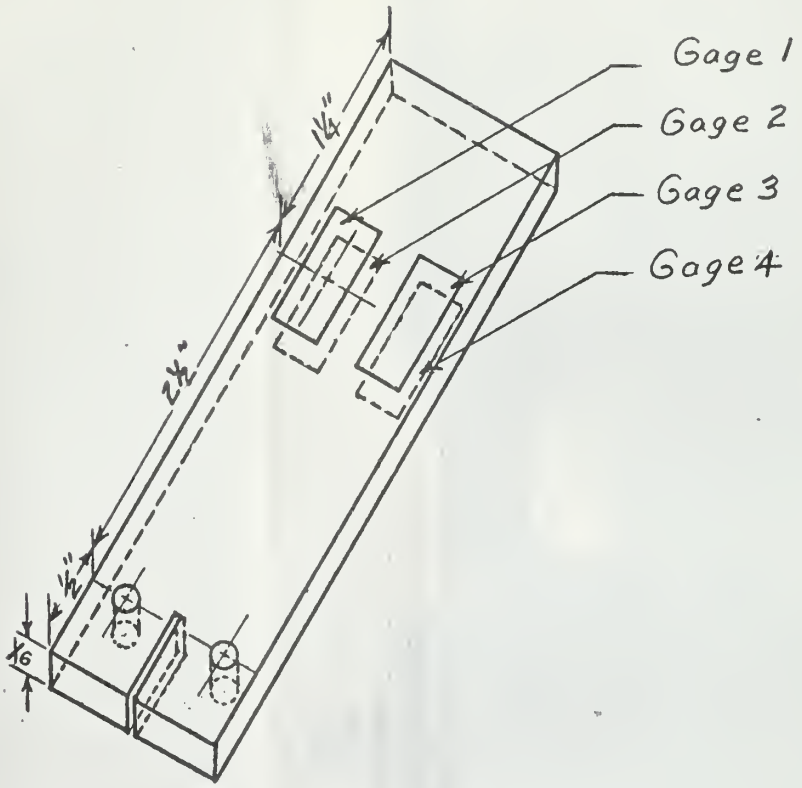

Friction Beam

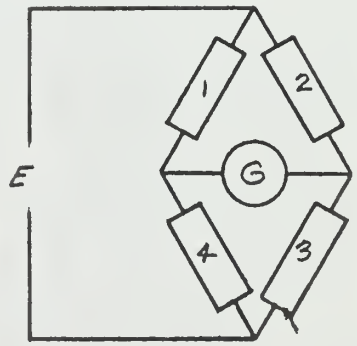

Strain Gage Circuit

FIGURE 6 FRICTION BEAM AND STRAIN GAGE CIRCUIT

FIGURE 7, SURFACE ANALYZING EQUIPMENT

4. Specimens

Figure 8 is a photograph of a typical pair of specimens, and figure 9 displays their dimensions. Tables I, II and III give the specimen's compositions and physical properties. Figure 10 is a special chrome plated specimen. All of the specimens were received from NEES, Annapolis, Maryland.

The metal specimens and spindle had to be very carefully made to hold total run-out at the surface of the metal specimen at a minimum. Even the small run-out achieved (.0001 to .0005 in.) affects the wear depth measurement; however, it can be distinguished from wear as explained in Appendix I.

The surface roughness was determined by averaging surface analyzer measurements at various spots on each specimen. Figures 11 through 16 are surface roughness traces for the specimens as taken from the analyzer instruments.

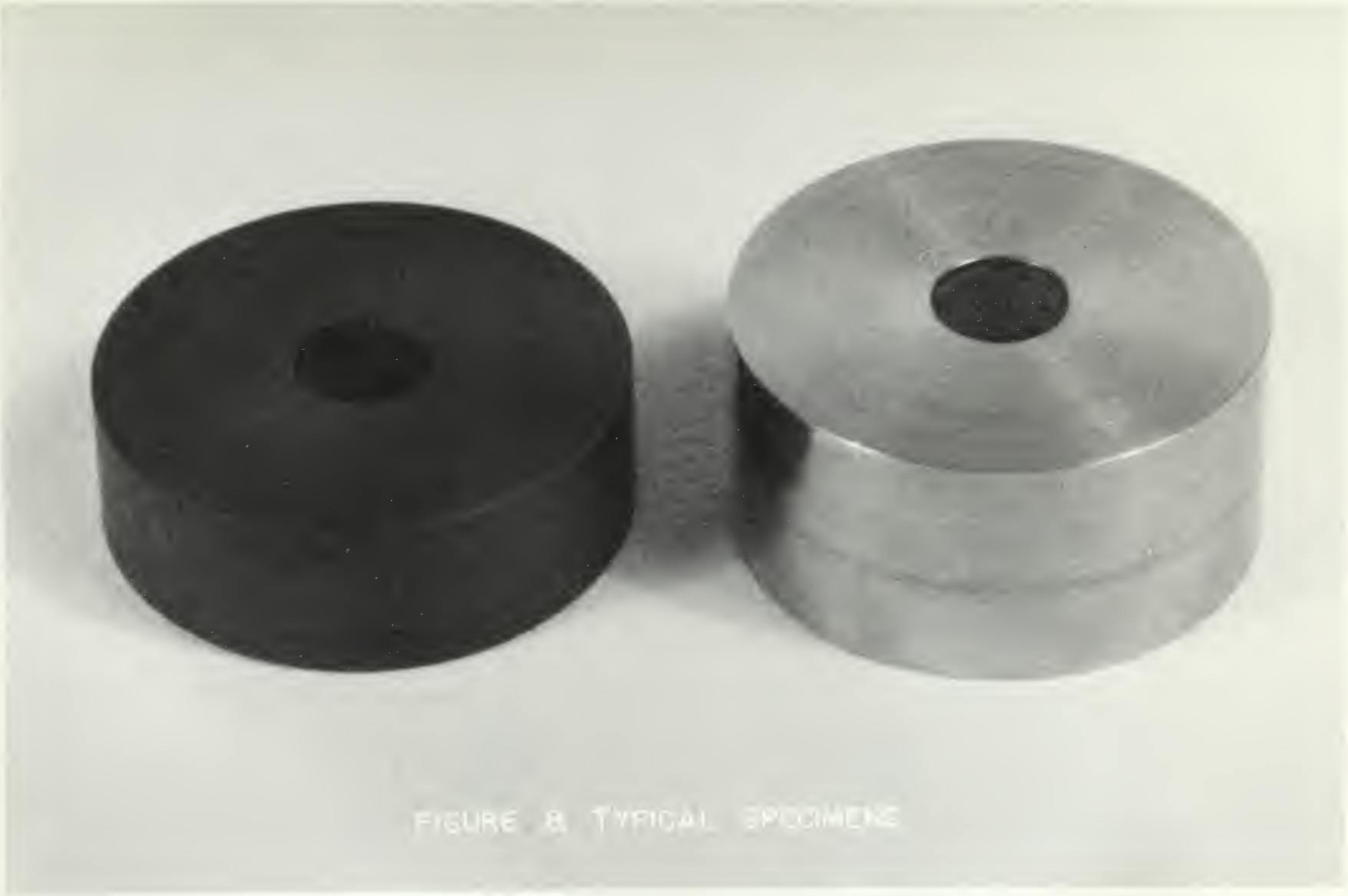

FIGURE 8 TYPICAL SPECIMENS

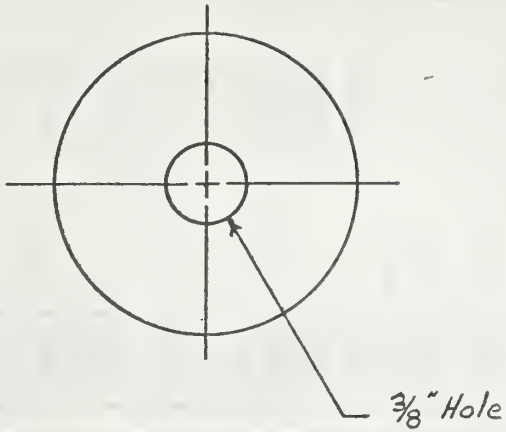

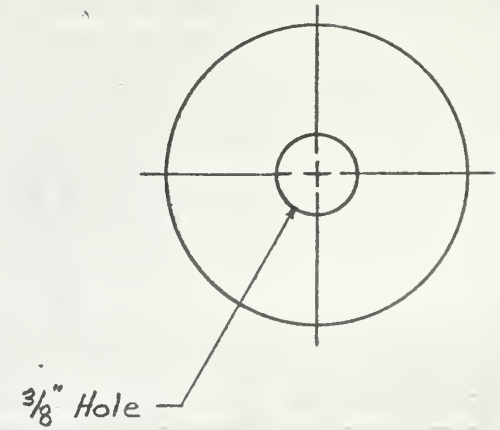

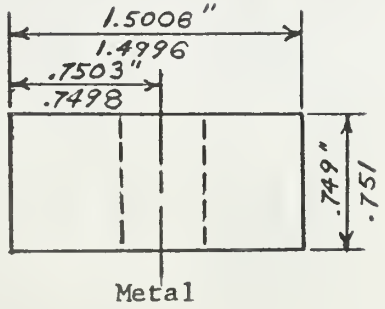

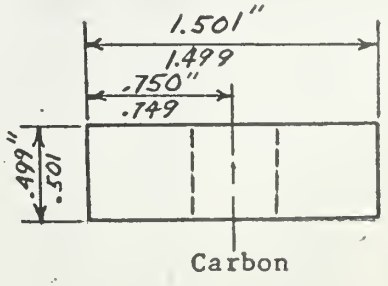

FIGURE 9 SPECIMEN DIMENSIONS

Table I

Metal Specimen Composition

Design.	Material	Preparation	Composition (%)
DSQ	Stellite	Cast	Ci 67, Cr 28, W 4, C 1
DSY	S-Monel	Cast	Cu 29, Si 3.87, Fe 2.11, Mn .78, Ni = Balance
DSZ	Cupalloy	Cast	
DSR-4	Tin-Bronze	Cast	Cu 87.9, Sn 6.41, Pb 1.3, Ni .16, Fe .02
DSS	Al-Bronze	Cast	Cu 82.3, Ni 4.4, Fe 2.9, Mn .12, Al = Balance
DSR-9	Chrome Plated Tin-Bronze	--	--

Table II

Metal Specimen Properties

Design.	Tensile Strength (psi)	Yield Strength (psi)	Brinell Hardness	Elongation (%)	Surface Roughness RMS
DSQ	120,000	118,000	440	1	2-4
DSY	90-145,000	70-115,000	285	4	6-10
DSZ	47-50,000	35,000	100-120	25-30	4-6
DSR-4	34,000	17,000		20	2-5
DSS	--	25-45,000	154	5-30	6-12
DSR-9	--	--	--	--	10-16

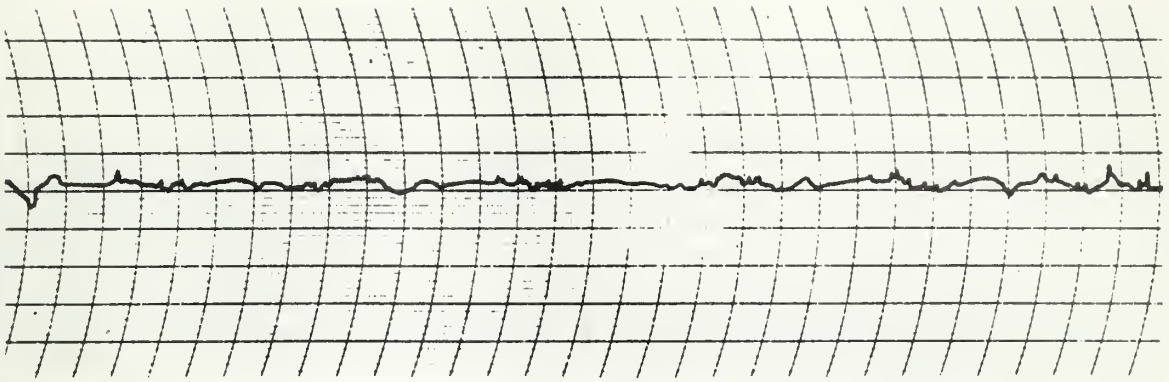

FIGURE 11 STELLITE SURFACE ROUGHNESS TRACE

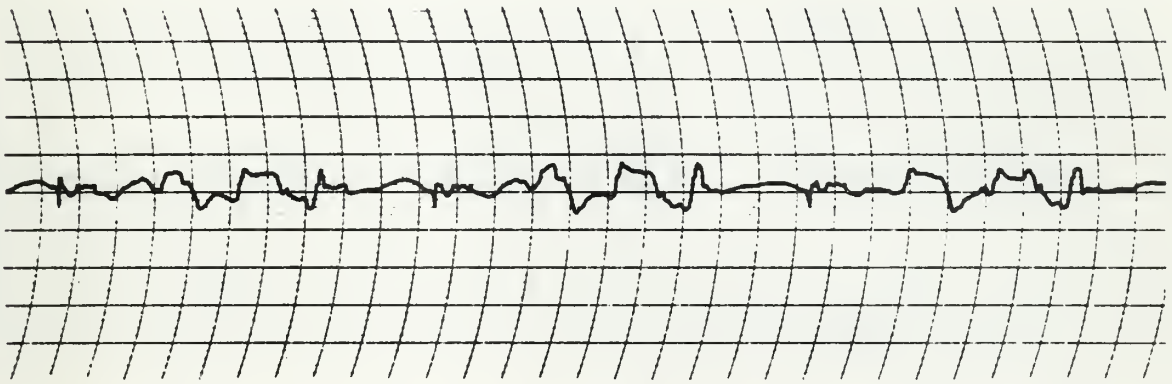

FIGURE 12 S-MONEL SURFACE ROUGHNESS TRACE

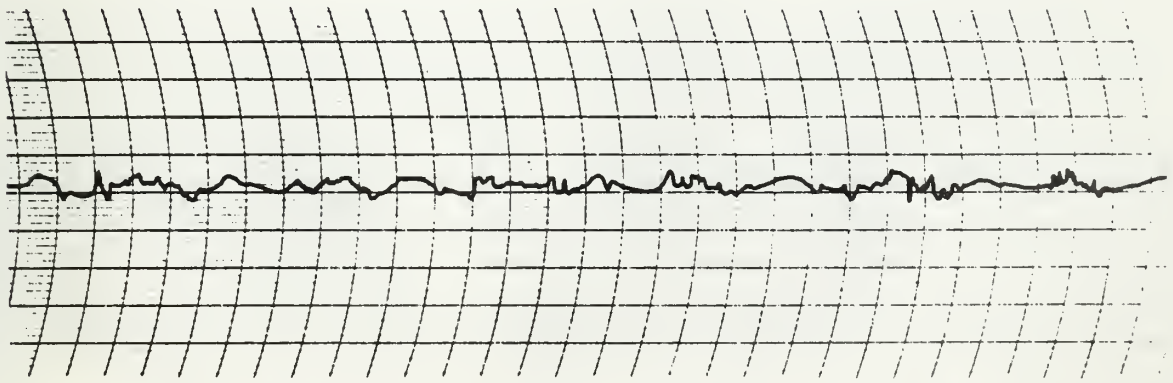

FIGURE 13 CUPALLOY SURFACE ROUGHNESS TRACE

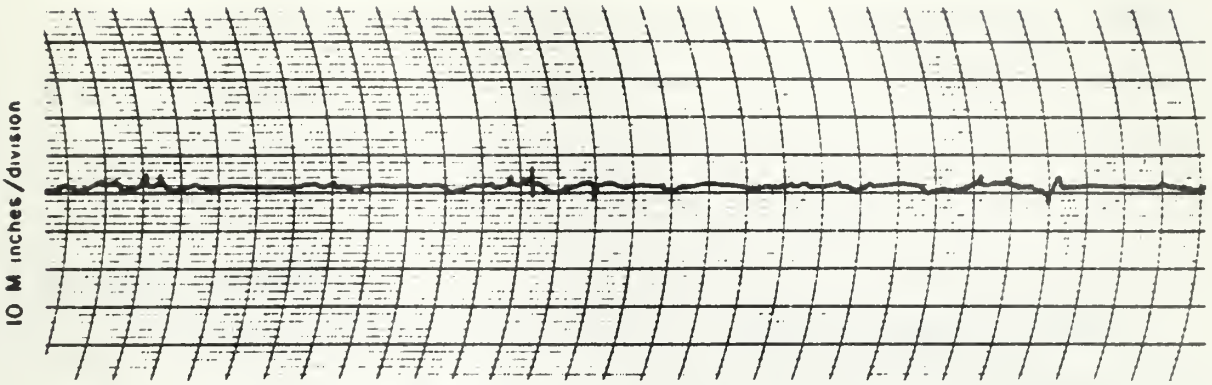

FIGURE 14, TIN-BRONZE SURFACE ROUGHNESS TRACE

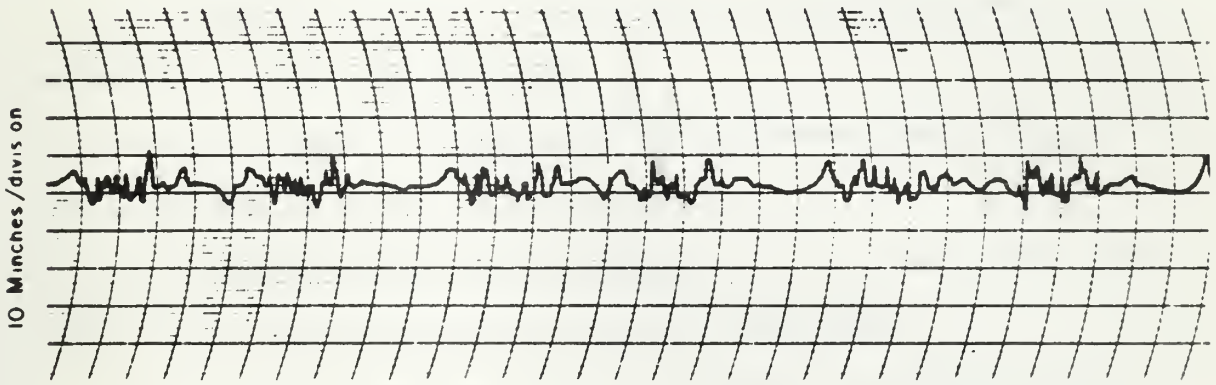

FIGURE 15, AL-BRONZE SURFACE ROUGHNESS TRACE

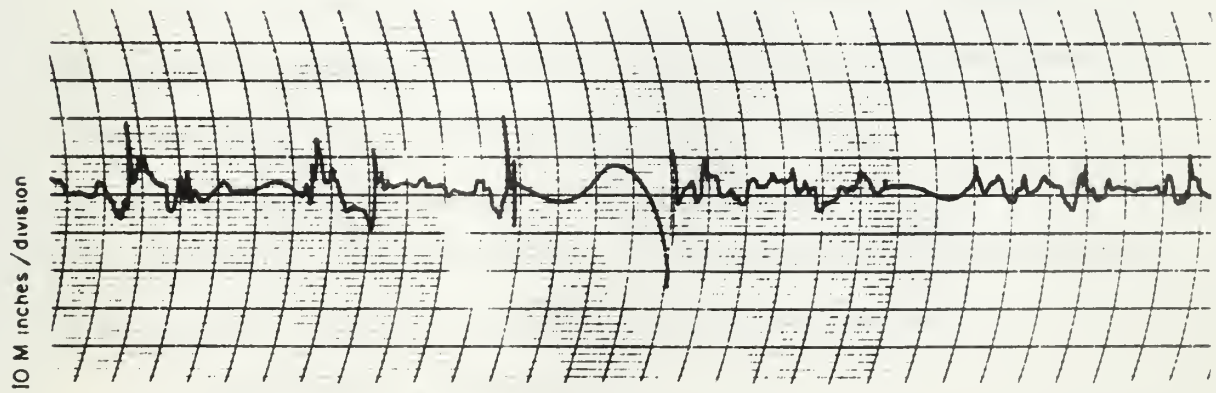

FIGURE 16, CHROME PLATE SURFACE ROUGHNESS TRACE

5. Procedure

Two different procedures were used during testing; one common to all constant load tests, and one common to all of the adjusted constant-contact-pressure tests. For both procedures, the specimens were cleaned with triethel-chloride, and the instruments allowed to warm up for one hour prior to commencing a run.

Constant Load Tests

1. Prior to making an actual run, a constant signal was sent to the instruments for the time duration of a test in order to insure there was no drift in the instruments.

2. After the specimens were secured in place, the counter-weight was adjusted to balance the apparatus.

3. The spindle was moved, with the micrometer bench, to place the metal specimen in contact with the carbon.

4. All lost motion in the bearings and linkage deflections were taken up by applying the test load to the weight pan.

5. The transformer was nulled by adjusting the micrometer and observing the DDI meter.

6. Desired sensitivity was set on the DDI and X-Y recorder. It was checked by displacing the core .001", and observing the number of divisions displaced by the recording pen.

7. Lubricant was applied to the specimens, and the X-Y recorder pen observed for displacements due to thermal expansion or contraction; if no movement occurred, thermal equilibrium was assumed.

8. Both recorders were started.

9. The test was commenced by starting the drive motor; test duration was between 10-15 minutes.

10. At the termination of the test, the motor was stopped and the recorder pen was observed for displacement due to thermal contraction. If none was observed, thermal equilibrium throughout the test was assumed.

11. The wear scar diameter was now measured with the microscope, and calculations were made as outlined in Appendix I.

Some constant load tests were made at various speeds to observe the effects on friction. For these tests, the Constant Load Procedure was followed except for speed changes. The specimens were run together at 3000 RPM. The Esterling Angus Recorder was stopped and the speed changed by adjusting the Vickers transmission while observing the counter. The recorder was then turned on again. The motor was not stopped during the operation, and speed adjustment took about 5-10 seconds.

Adjusted Constant-Contact-Pressure Tests

1. Procedures 2 through 4 were carried out as in the Constant Load Tests.

2. The lubricant and motor were started; a 15 second run was made.

3. The motor was stopped, and the wear scar diameter measured with the microscope. The measurement was accomplished by breaking surface contact, and placing the carbon specimen and microscope as shown in figure 3.

4. The carbon specimen was swung back into running position and sufficient load added to obtain the desired contact pressure.

5. Lubricant and motor were again started for another period of time. Procedures 3 and 4 were repeated, and another running period commenced. This procedure was followed until a 15-20 minute run was completed.

6. Calculations were made as outlined in Appendix 1.

Calibration

Calibration of the depth recording instruments was done as indicated in the above procedure. The friction beam was calibrated by suspending 0.1 pound weights from the beam and observing the recording-pen displacement.

6. Description of Graphical and Tabular Results

Figures 17 through 22 are a graphical display of wear data obtained for various combinations of carbon and metal specimen Total volume worn away vs. time is plotted. Since the properties of the carbon specimen affect the wear results more than those of the metal specimens, various metals are compared for a particular carbon. Wear rate may be obtained from the slopes of these curves. Table IV contains the coefficients of friction for the runs represented by figures 17 through 22 along with some additional runs.

Figures 23 and 24 are friction traces as recorded with the apparatus; they compare the two types of curves obtained.

Figures 25 and 26 are photomicrographs which were taken of wear spots on the same carbon specimen. Figure 26, a fraction of a wear spot, was taken at the same magnification as figure 25 which shows the entire spot. Figure 25 was taken after 12 minutes of running time and is a normal wear spot; figure 26, taken after a few seconds of running time, is the result of accelerated wear.

Figure 27 is a plot of total volume worn away vs. time, for different load levels at 3000 RPM; CC carbon and DSQ metal specimens were used.

Figure 28 is a plot of total volume worn away vs. time, for various contact pressure levels. The CC carbon and DSQ metal specimens were used.

Figure 29 is a plot of total volume worn away vs. total sliding distance for different speed levels with a constant 2 lb. load. The curves were drawn to depict the dependence of wear rate on sliding velocity.

Figure 30 is a friction trace showing the effects of speed changes on friction force; Table V contains the various coefficients of friction for this run.

Figure 31 shows various friction traces at different load levels; Table VI contains the coefficients of friction for these runs.

All of the tables of coefficients of friction contain an initial value and an average or steady value.

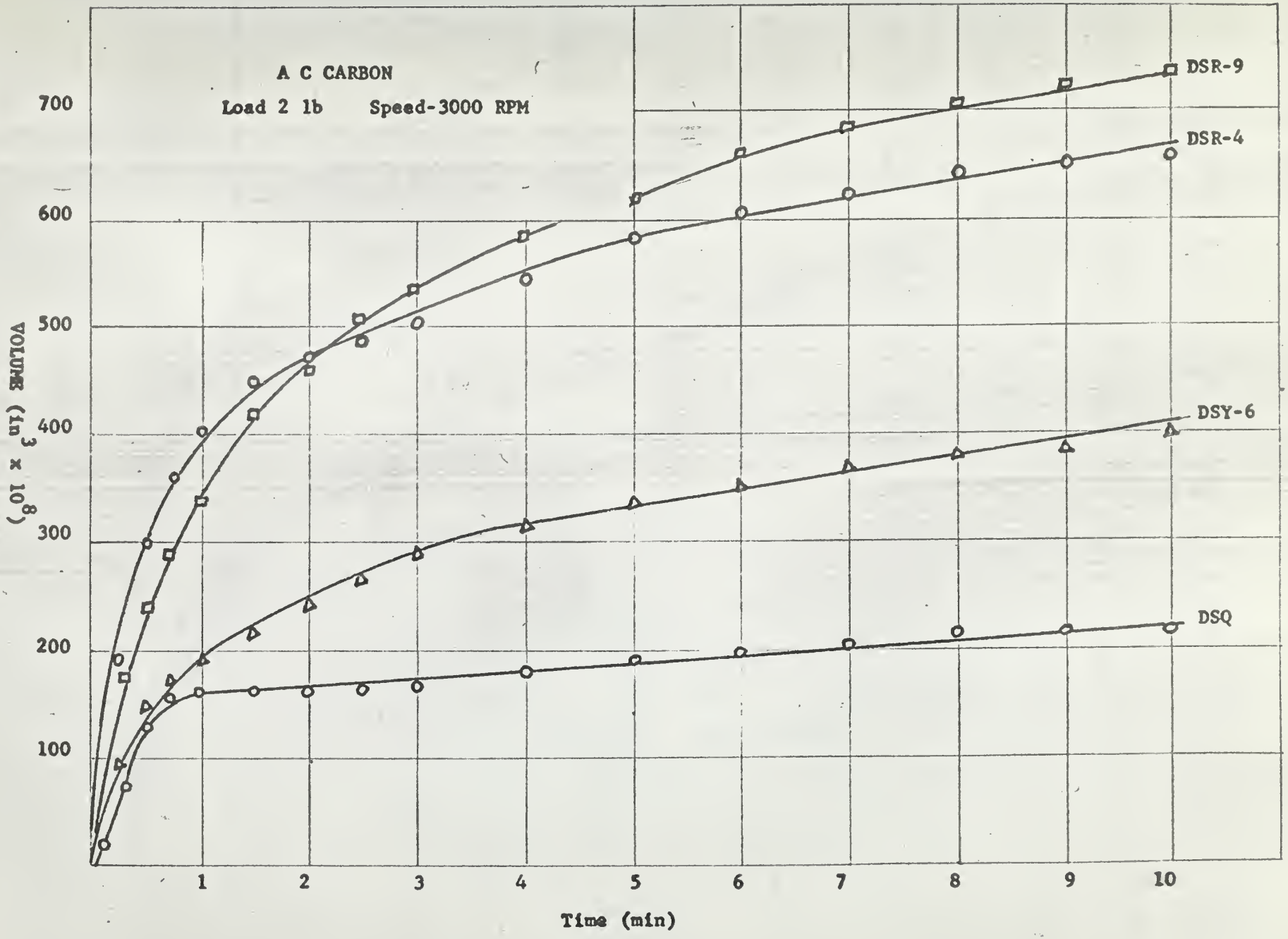
A C CARBON
Load 2 lb Speed-3000 RPM
DSR-9
DSR-4
DSY-6
DSQ
700
600
500
400
300
200
100
VOLUME (in^3 x 10^8)
1
2
3
4
5
6
7
8
9
10
Time (min)

FIGURE 17

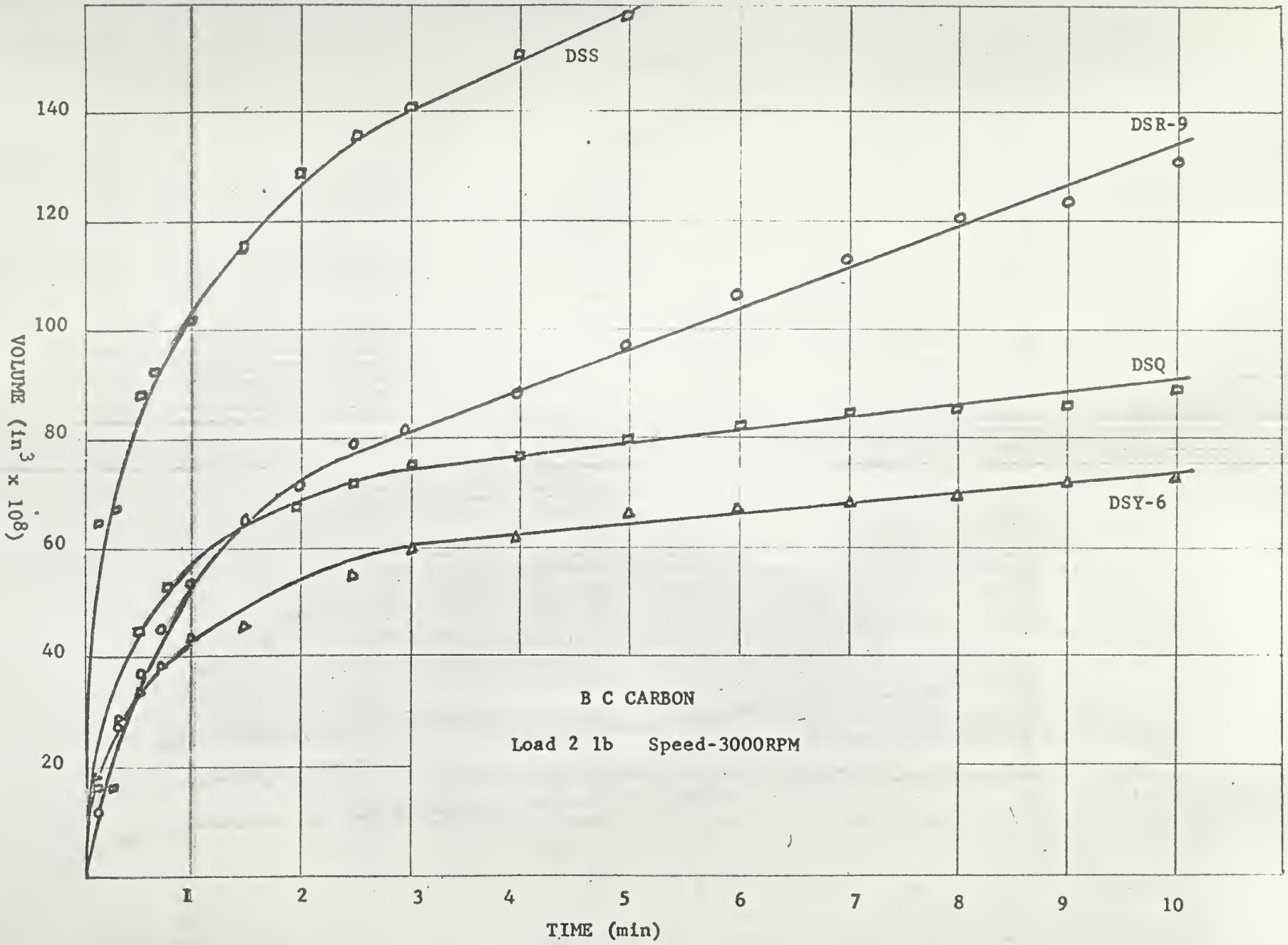
DSS
DSR-9
DSQ
DSY-6
B C CARBON
Load 2 lb Speed-3000RPM
VOLUME (in^3 x 10^8)
TIME (min)
20
40
60
80
100
120
140
1
2
3
4
5
6
7
8
9
10

FIGURE 18

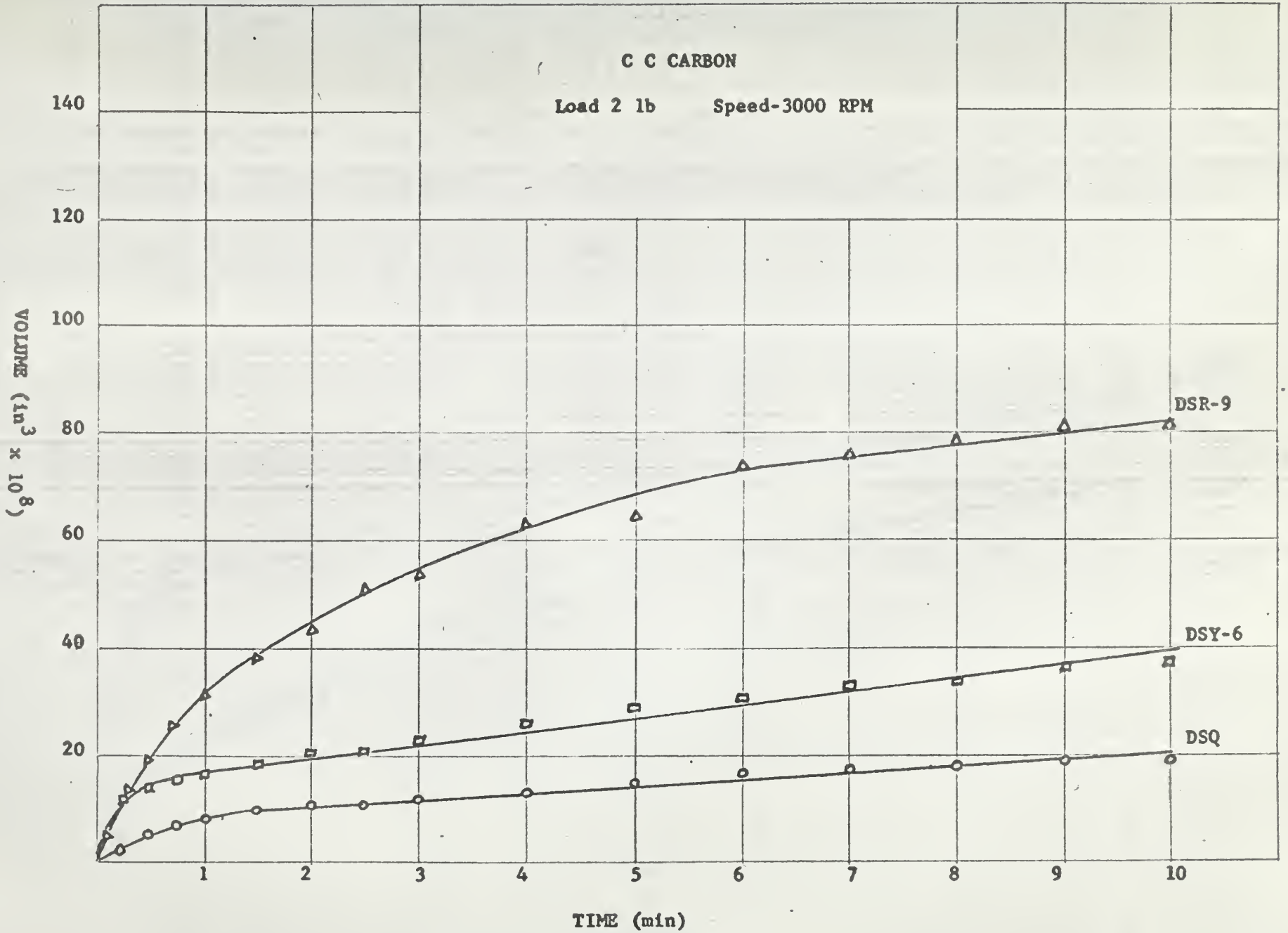
C C CARBON
Load 2 lb Speed-3000 RPM
140
120
100
80
60
40
20
VOLUME (in^3 x 10^8)
1
2
3
4
5
6
7
8
9
10
TIME (min)
DSR-9
DSY-6
DSQ

FIGURE 19

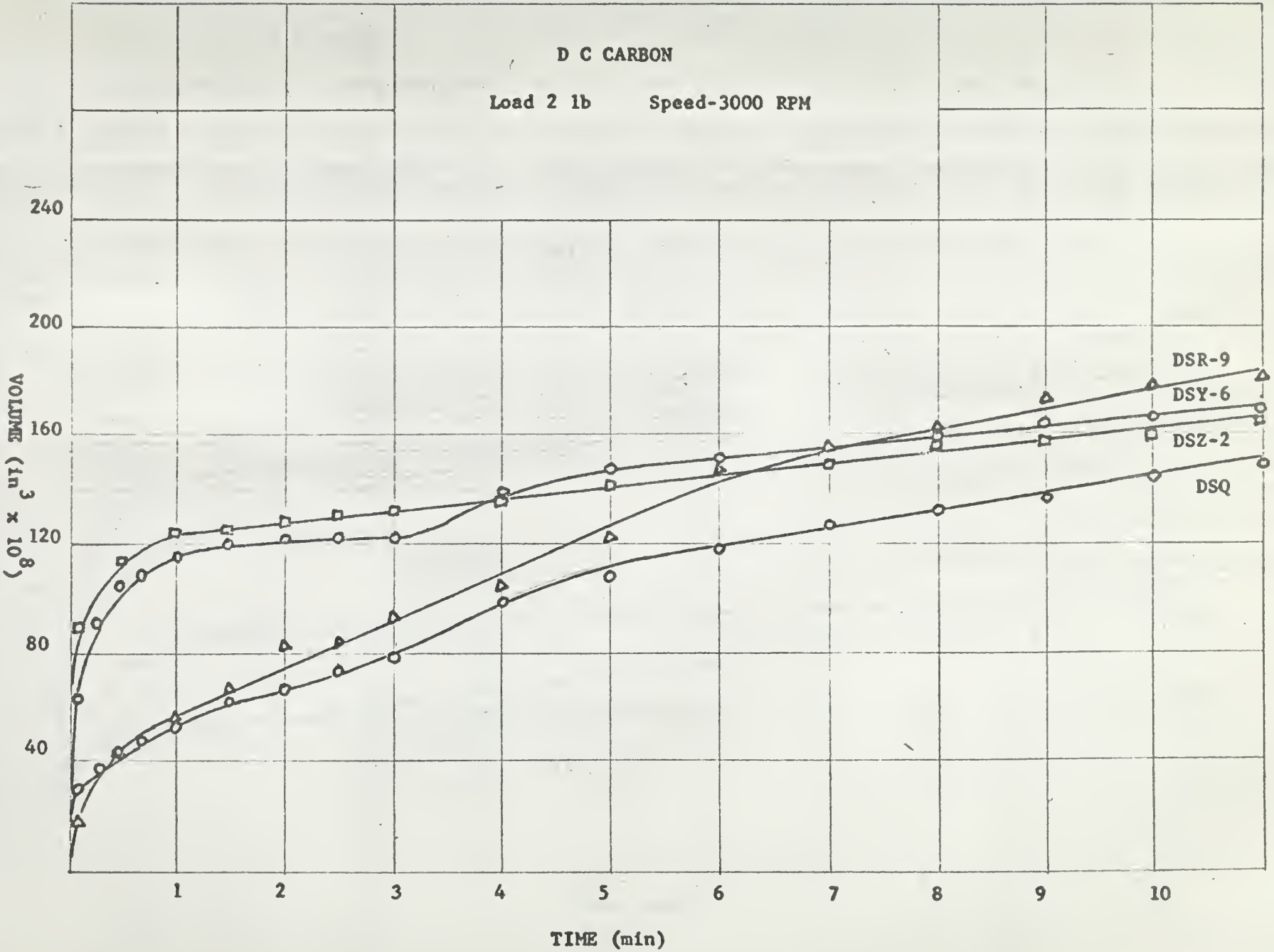
D C CARBON
Load 2 lb Speed-3000 RPM
240
200
160
120
80
40
VOLUME (in^3 x 10^8)
1
2
3
4
5
6
7
8
9
10
TIME (min)
DSR-9
DSY-6
DSZ-2
DSQ

FIGURE 20

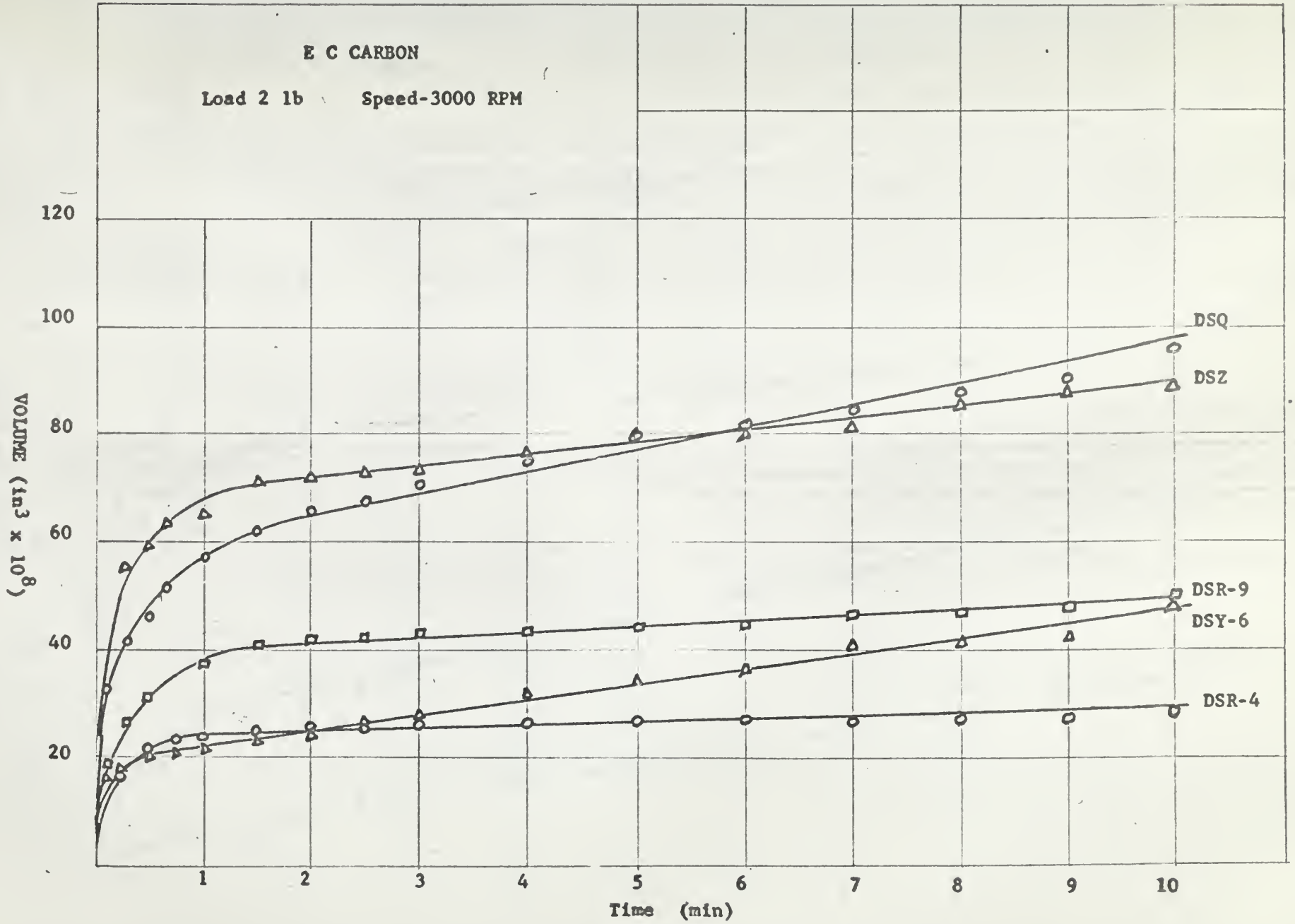
E C CARBON
Load 2 lb Speed-3000 RPM
VOLUME (in3 x 10^8)
120
100
80
60
40
20
1
2
3
4
5
6
7
8
9
10
Time (min)
DSQ
DSZ
DSR-9
DSY-6
DSR-4

FIGURE 21

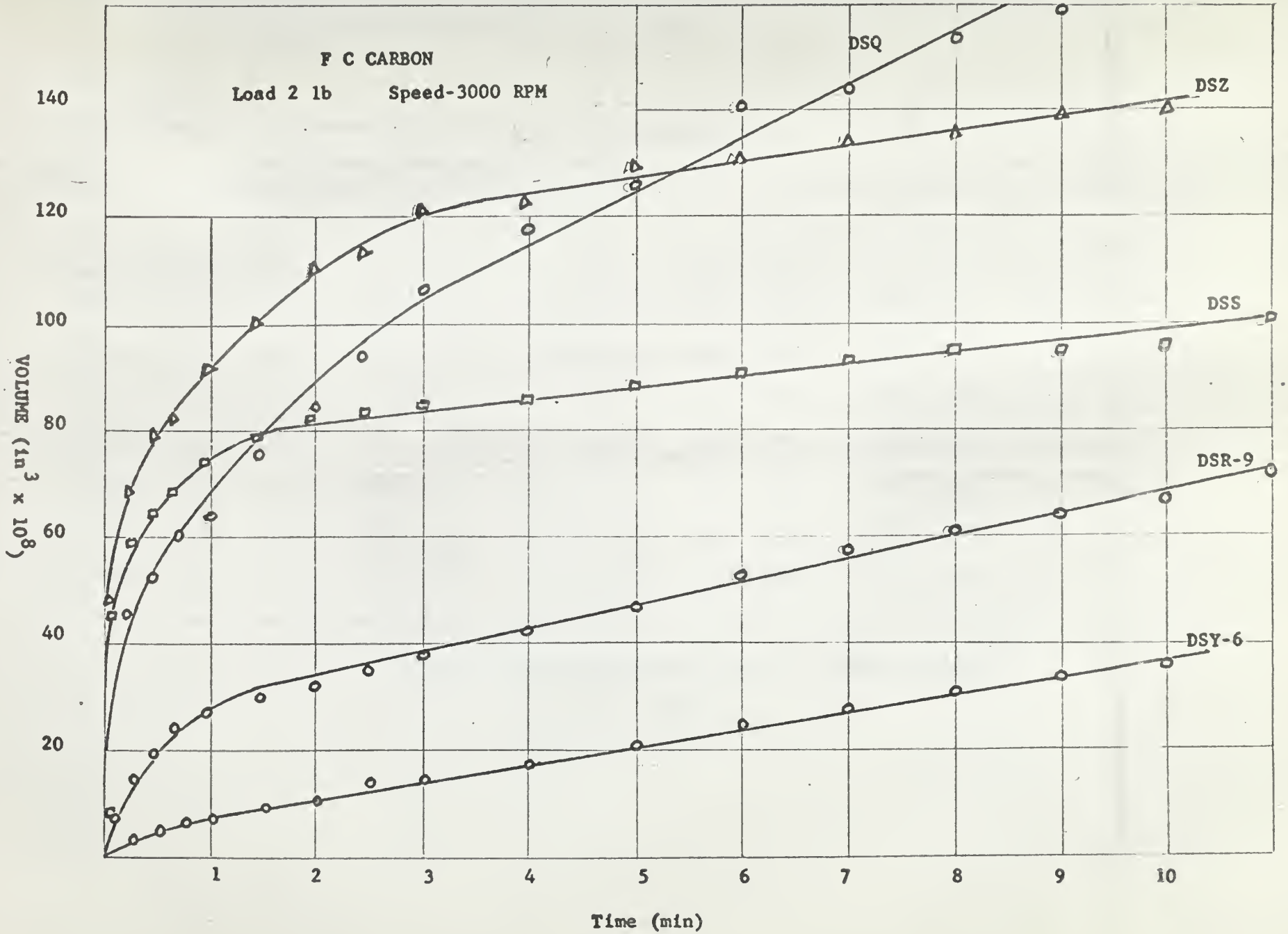
F C CARBON
Load 2 lb Speed-3000 RPM
DSQ
DSZ
DSS
DSR-9
DSY-6
VOLUME (1n^3 x 10^8)
140
120
100
80
60
40
20
1
2
3
4
5
6
7
8
9
10
Time (min)

FIGURE 22

CARBON SPECIMENS

Metal Spec.	AC Init. Frict.	AC Avg. Frict.	BC Init. Frict.	BC Avg. Frict.	CC Init. Frict.	CC Avg. Frict.	DC Init. Frict.	DC Avg. Frict.	EC Init. Frict.	EC Avg. Frict.	FC Init. Frict.	FC Avg. Frict.
DSZ	.[illegible]	.015	.173	.146	.079	.067	.065	.085	.089	.089	.085	.100
DSS	.039	0	-	-	-	-	.039	.023	.058	.065	.050	.065
DSR-4	.065	.065	.131	.027	.111	.058	.065	.062	.065	.065	.073	0.65
DSY-6	.065	.037	.069	.062	.063	.069	.085	.065	.077	.069	.116	.096
DSQ	.054	.004	.039	.004	.063	.034	.065	.023	.050	.019	.050	.019
DSR-9	.050	.004	.054	.012	.062	.034	.112	.089	.077	.065	.065	.004

COEFFICIENTS OF FRICTION: LOAD 2 LBS, SPEED 3000 RPM

Table IV

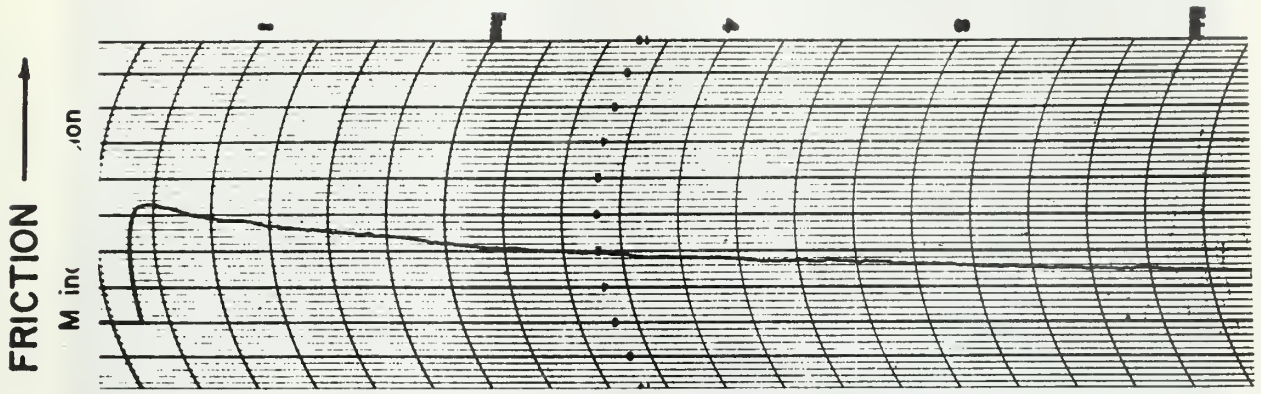

FIGURE 23, TYPICAL FRICTION TRACE

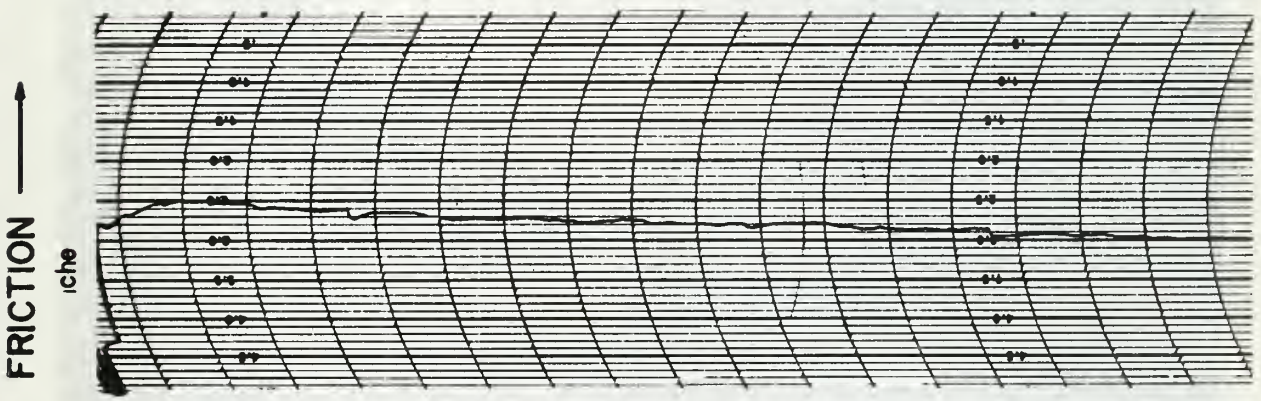

FIGURE 24, TYPICAL FRICTION TRACE

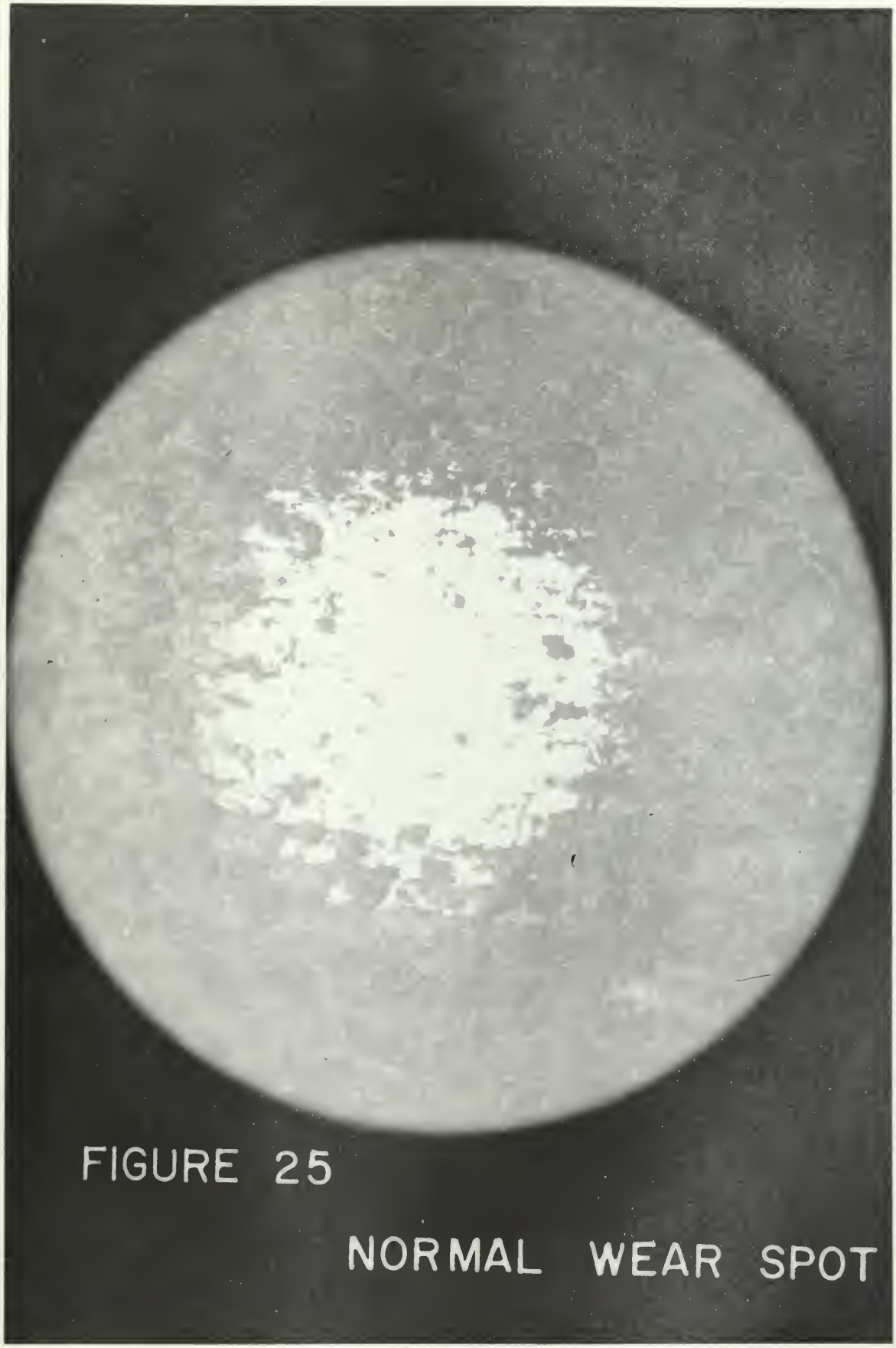

FIGURE 25

NORMAL WEAR SPOT

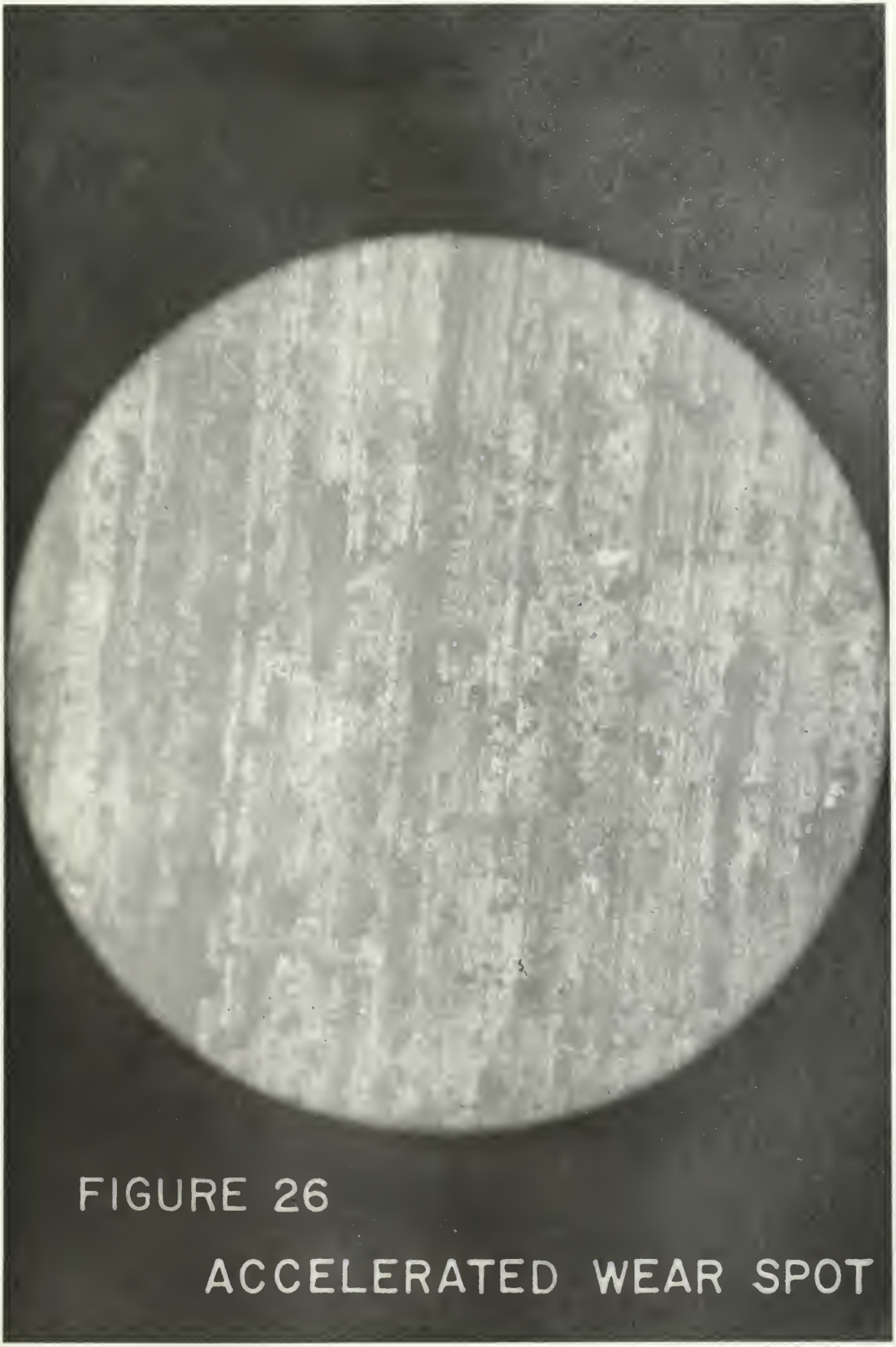

FIGURE 26

ACCELERATED WEAR SPOT

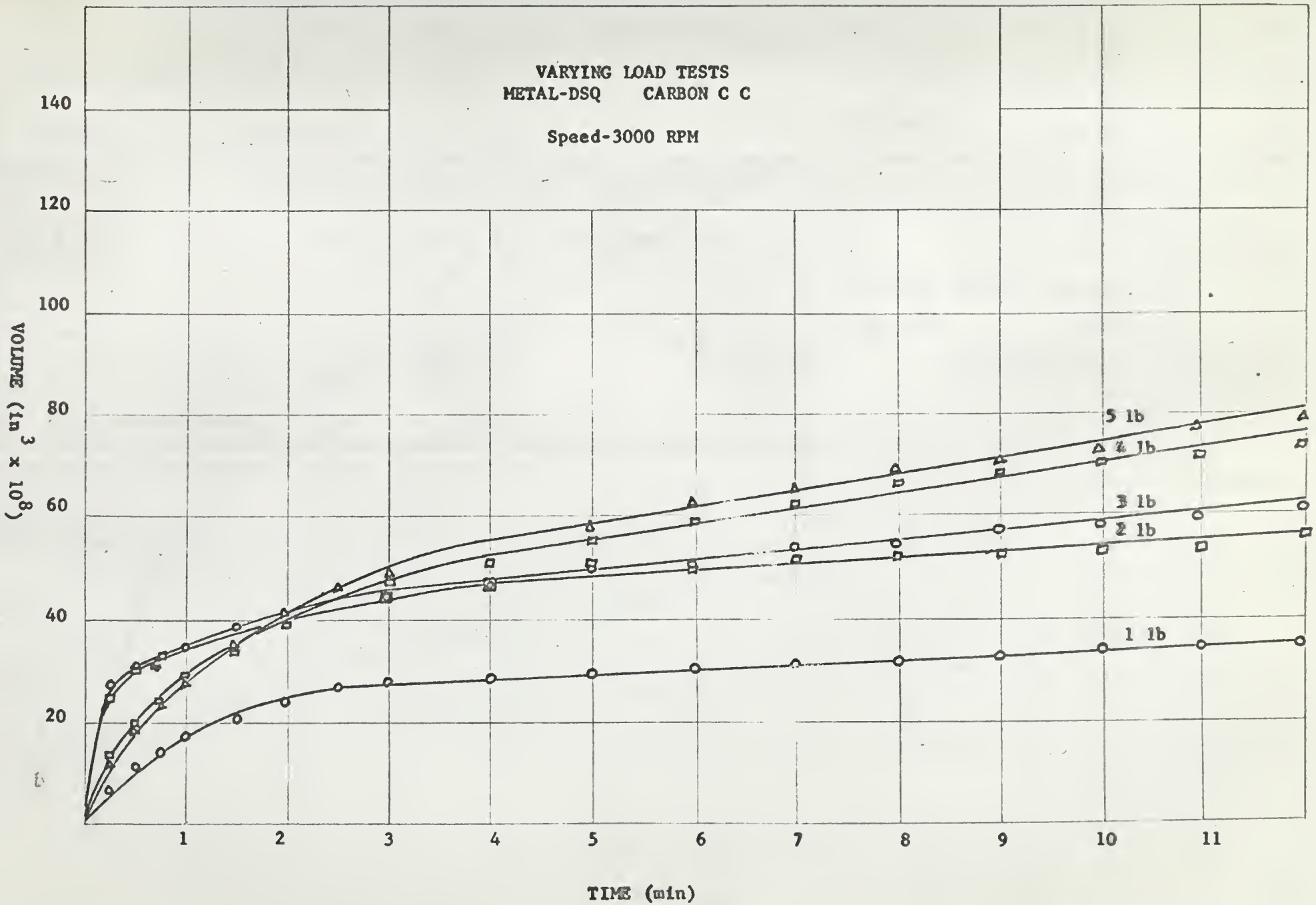
VARYING LOAD TESTS
METAL-DSQ CARBON C C
Speed-3000 RPM
VOLUME (in^3 x 10^8)
140
120
100
80
60
40
20
1
2
3
4
5
6
7
8
9
10
11
TIME (min)
5 lb
4 lb
3 lb
2 lb
1 lb

FIGURE 27

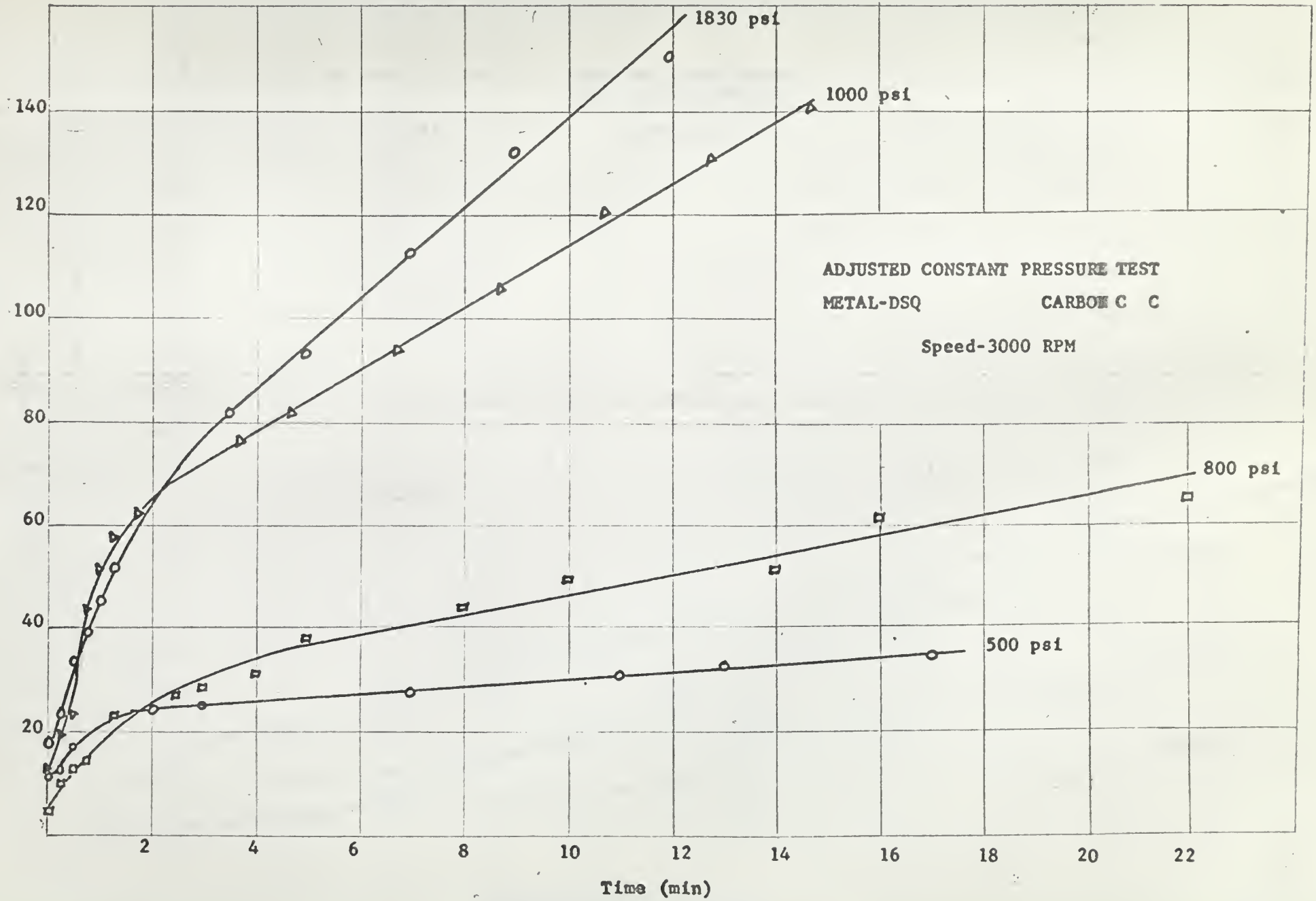
1830 psi
1000 psi
800 psi
500 psi
ADJUSTED CONSTANT PRESSURE TEST
METAL-DSQ CARBON C C
Speed-3000 RPM
VOLUME (in^3 x 10^8)
Time (min)
20
40
60
80
100
120
140
2
4
6
8
10
12
14
16
18
20
22

FIGURE 28

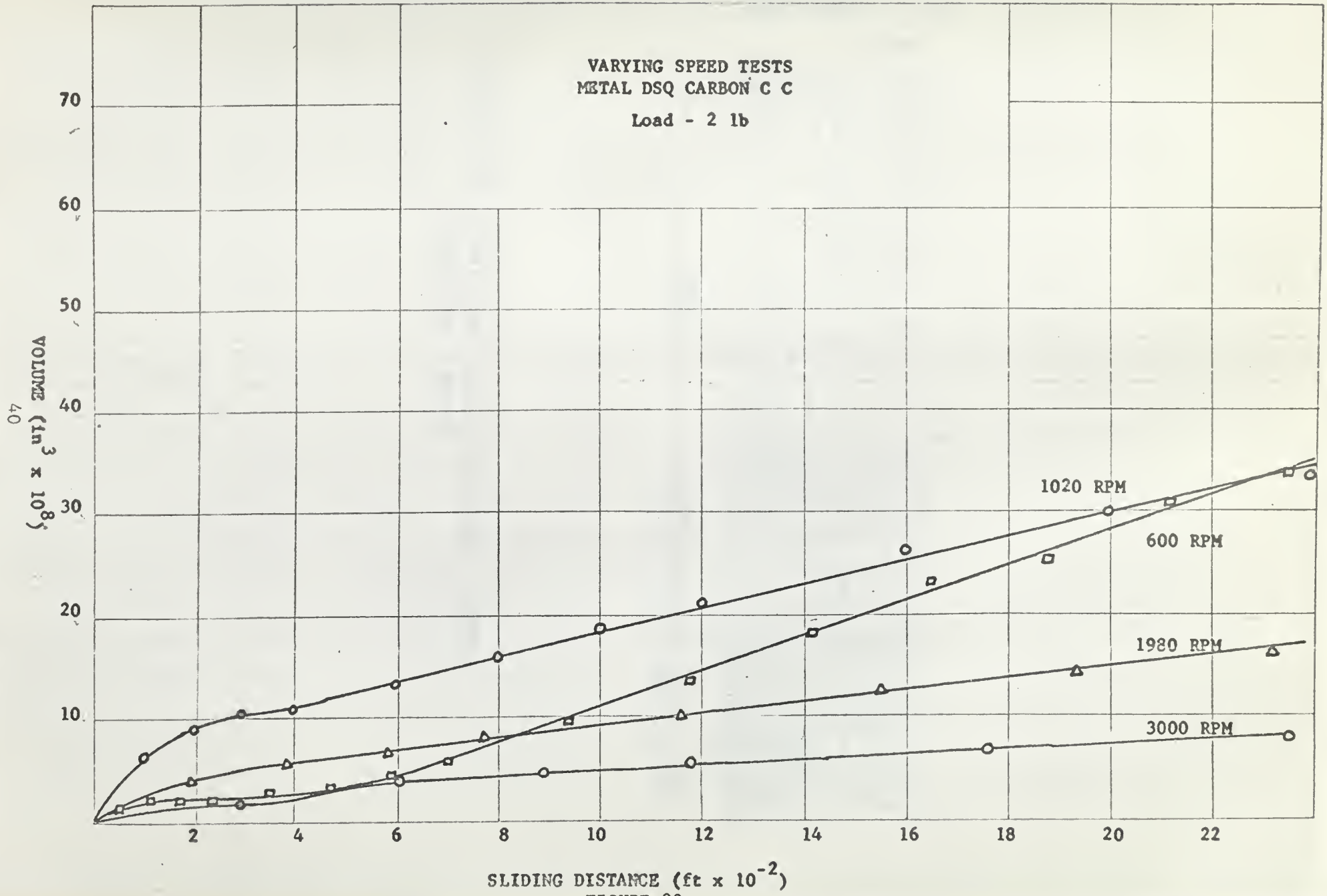
VARYING SPEED TESTS
METAL DSQ CARBON C C
Load - 2 lb
70
60
50
40
30
20
10
VOLUME ($in^3 \times 10^8$)
1020 RPM
600 RPM
1980 RPM
3000 RPM
2
4
6
8
10
12
14
16
18
20
22
SLIDING DISTANCE ($ft \times 10^{-2}$)

FIGURE 29

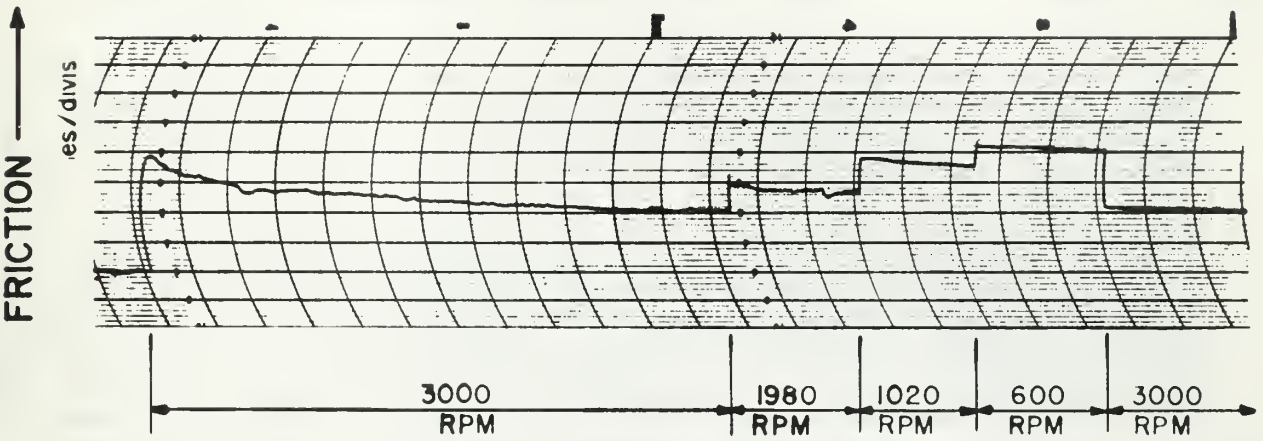

FIGURE 30, CONSTANT LOAD; VARYING SPEED
FRICTION TRACE

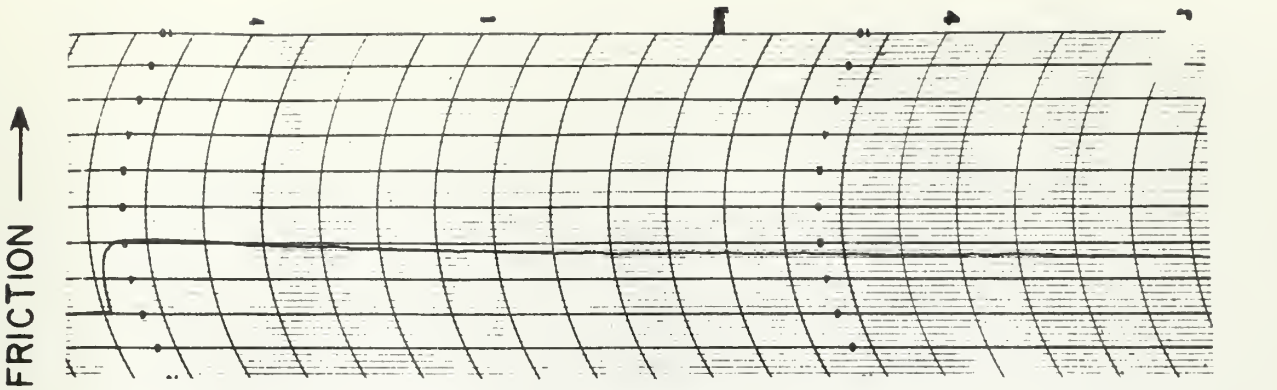

FIGURE 31A FRICTION TRACE; 1 lb. LOAD

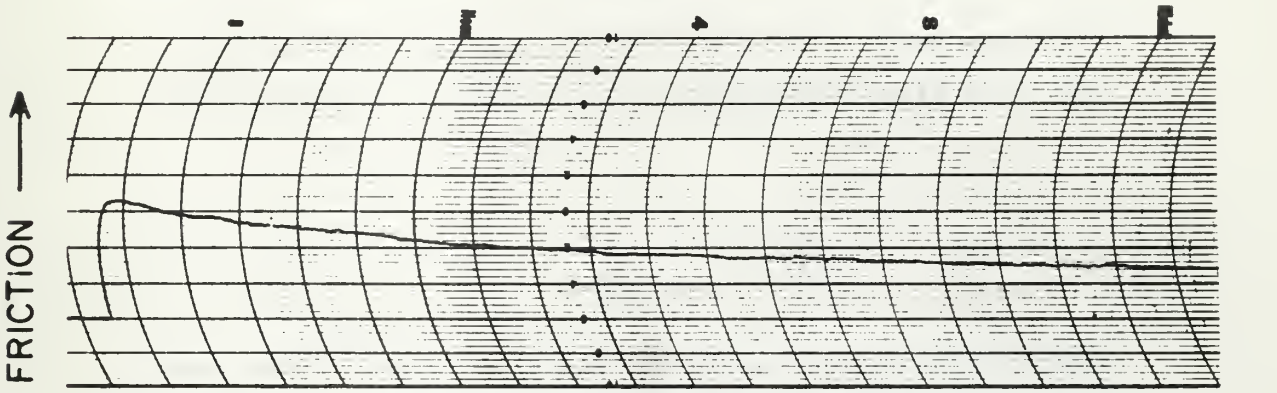

FIGURE 31B FRICTION TRACE; 2 lb. LOAD

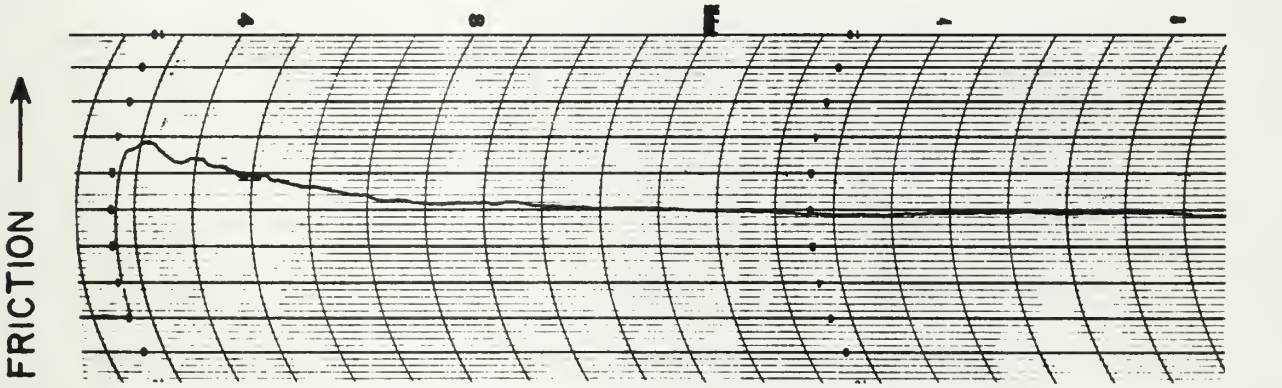

FIGURE 31C FRICTION TRACE; 3 lb. LOAD

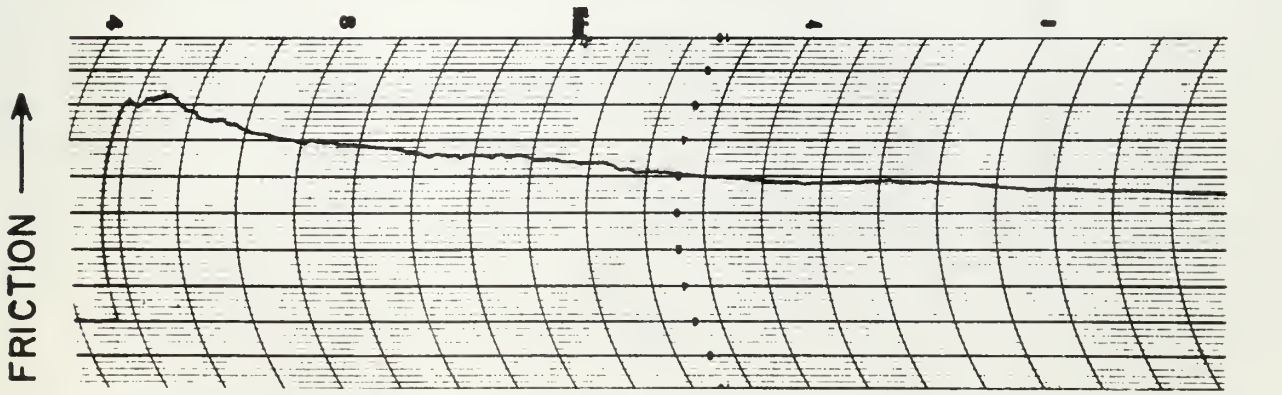

FIGURE 31D FRICTION TRACE; 4 lb. LOAD

Table V

Load (lb.)	Coefficient of Friction	
	Initial	Average
1	.077	.062
2	.063	.034
3	.061	.038
4	.056	.036

Coefficients of Friction CC Carbon-Stellite; Speed 3000 RPM

Table VI

Speed (RPM)	Coefficient of Friction	
	Initial	Average
600	-	.081
1021	-	.069
1980	-	.054
3000	.073	.038

Coefficients of Friction CC Carbon-Stellite; Load--2 lbs.

7. Discussion of Results

The results of this investigation have been displayed in graphic and tabular form. The investigation was carried out in two phases:

Phase one. This phase concerns the testing of various combinations of carbon and metal specimens.

Phase two. This phase concerns a more detailed investigation of the friction-wear characteristics common to the carbon and metal specimen selected from the results of phase one. Phase-two includes:

a) constant load tests,

b) adjusted constant contact pressure test, and

c) varying speed tests.

Phase-one curves are included to display the net volume worn away vs. time results for nearly all of the material combinations (figures 17 through 22). The coefficients of friction are listed in tabular form (table IV). The following points are evident from the results of phase one.

1. The wear curves for all runs have a run-in period followed by a nearly constant wear rate.

2. Carbons CC and FC have the best wear characteristics (lowest wear rate), where as, AC and DC have the worst. From Table III, it can be seen that the CC and EC carbons have a relatively high hardness, and that the CC carbon has a low modulus of elasticity. It appears that these properties, especially hardness, can serve as a selection criterion to obtain low wear rates.

3. Stellite and S-monel are the best mating materials from the standpoint of least wear rate.

4. Considering all runs, stellite had the lowest coefficients of

friction associated with it.

The nearly constant wear rate found has also been noted in tests by Holm, Burwell and Strang, Archard and others. The above investigators used equation -1- to justify their results; it appears that a similar relation might apply for this investigation. This would, of course, imply that the wear rate is dependent on normal load and independent of contact pressure.

Carbons CC and EC are two of the harder carbons, (see Table III) and when mated with a hard mating-face such as stellite, display good wear characteristics. Hardness is considered important in selecting most wear resistant materials. This selection criterion is also suggested by Lyddon and Hurden for carbons used in high pressure seal application.(11)

Friction curves had two characteristic shapes as illustrated by a comparison of figures 23 and 24. A further comparison of the friction and wear data reveals that the wear rate does not depend on the shape of the friction curves-high friction does not necessarily imply high wear rates as might be expected. Similar results have been obtained in carbon brush experiments by Millet.(12) In his investigations, wear rate varied largely with the ability of the carbon to absorb moisture.

When the DSS specimen was mated with either BC or CC carbon there was always extremely accelerated wear. Figure 25 is a normal wear scar; figure 26 is a small portion of a scar resulting from accelerated wear. Both photomicrographs were taken with the same magnification. There is an obvious difference in the brightness of the spots, also score lines

can be seen in the accelerated wear scar. There seems to be a natural affinity between the BC and CC carbons and the DSS specimen resulting in strong adhesion welds between the surfaces. These welds cause extremely high friction and high wear rates.

There were a few cases in which results were not obtainable because friction heat expanded the specimens so that the recorded traces could not be accepted as representing the true wear depth. In all of these cases the DSS, DSZ, or DSR specimens were involved--most times the DSS specimen. These metals are softer than the other metal specimens; all contain more than 82% copper, and have the largest coefficients of thermal expansion. Usually, they produced high wear rates. It is not believed that these materials would have been selected for good wear characteristics had they been given more consideration.

The carbon specimen and stellite were chosen for more detailed testing in phase-two.

Phase-two curves are included for the constant load tests, and adjusted constant-contact-pressure tests. Friction data, at various load levels and speeds are also tabulated. The following points are evident from the results of phase two.

1. Wear rate curves vary regularly with contact pressure.
2. Friction force increases with decreasing speed.
3. The time rate of wear increases with decreasing speed.
4. The above results along with that gathered in phase-one lead to the conclusion that carbon wear phenomena as experienced in these tests, are dependent upon boundary lubrication.

A comparison of the constant load curves, figure 27, and the adjusted constant-contact-pressure curves, figure 28, leads to the conclusion

that wear rate is more dependent on contact pressure than on normal load. Further evidence of this dependence may be found by examining the data in Appendix II. It is seen that the constant pressure runs have a normal load increase of about three fold; yet, the wear curves remain very regular. It is also seen that the constant load runs have a rapid change of contact pressure initially; however, this rate soon decreases until there is a very slow change in pressure--so slow that the run becomes essentially a constant pressure run. These are the same type of results found by Dorinson and Broman. They present the argument that specimen geometry has led to the erroneous conclusion, by Holm, Burwell and Strang, Archard and other investigators, that wear rate is load dependent. Dorinson and Broman used an adjusted constant contact pressure method, as was used in this investigation, with a conical pin and disc apparatus to arrive at their experimental evidence.

It must be mentioned,before conclusions are drawn, that an examination of the constant load data in Appendix II reveals that those runs at higher loads had very high contact pressures throughout the entire run; yet, they had low wear rates compared with the higher-pressure adjusted constant-contact-pressure runs. This can be attributed to the effects of the testing procedure for the adjusted constant contact pressure runs on boundary film lubrication--if such a film were of importance in the testing. During the constant pressure testing, the surfaces were broken at short intervals for measurement of the wear scar. This destroyed any high temperature film at the contact surface so that when the surfaces were rematched, the film had to re-establish itself. At high pressures, the surfaces were broken more frequently for measurement, and the film recovery could have been more difficult; this would cause an increase in

wear rate.

Figure 25, a typical wear spot, has a very bright appearance indicating a polishing effect occurred. Polishing is usually accompanied by a layer of particles which afford boundary lubrication. Further evidence of boundary lubrication is provided by the friction and wear results for the constant load and varying speed runs (see figures 29 through 31, and tables V and V'). It was found that as speed decreased, friction and wear increased; as load increased, the frictional force increased, but the coefficient of friction decreased. Similar shapes of friction curves and friction variation with load and speed have been found by Halling,[10] and Milne, Scott and Mac Donald[13] with cross cylinder apparatus.

Conclusions

1. Considering all of the data, the importance of a boundary film is evident.

2. Carbon selection for high pressure seal applications should be based on hardness, and the carbon's ability to form a film under pressure.[2]

3. High rubbing speeds do not increase wear rate.

4. Frictional force does not increase linearly with load.

5. Frictional force does not vary regularly with wear rate.

6. A metal with high hardness should be used as a mating-face for a high hardness carbon.

7. Surfaces with fine finishes should be used in order to receive benefit from the boundary film.

8. A comparison of the data for the constant load test and the adjusted constant-contact-pressure test does not indicate a simple dependence on either load or contact pressure. There does, however, appear to be more dependence on pressure than load.

Recommendations

The problem of determining whether carbon wear is dependent on load or contact pressure, if either, has not been solved conclusively by this investigation. If it had not been necessary to break surface contact between the specimens during the adjusted constant-contact-pressure tests, the true effects of a boundary film could have been determined. The

---

[2]The fact that the carbon with the lowest wear rate, CC carbon, had the lowest modulus of elasticity along with highest hardness is also of interest.

machine work and instrumentation to adapt the apparatus to adjust the load automatically for constant pressure tests has been considered and a few runs actually attempted. The ideas are feasible but require considerable refinement. It is recommended that the cross cylinder apparatus be altered in the following ways to broaden and improve the results obtainable from it:

1. If figure 34 is considered, it is seen that the area of the wear spot varies almost linearly with the depth of wear. A weight pan, suspended from a sleeve bearing which slides on the load arm (lever arm K, figure 4) of the apparatus has been made. By using an Atcotran Class 6171 Servo Mechanism, the weight pan can be positioned on the lever arm by the depth of wear signal received from an LVDT as used in the investigation. This was actually accomplished. A simple mathematical relationship exists to determine the load to be added to the small pan to obtain the desired contact pressure. As wear occurs, the servo system acts on the depth of wear signal, and positions the weight pan to maintain a constant pressure. It was found, however, that with the existing apparatus, changing the load continuously caused a significant continual change in the linkage deformation;this, of course, caused erroneous depth of wear signals that affected the servo system, and the recorded wear results. The method should be studied further. Deformations might be reduced by re-designing the friction head and using brass instead of micarta. The bearings should be pre-loaded, or perhaps, pivot points used in lieu of bearings--there should be no lost bearing motion.

2. Thermocouples should be added to the carbon and metal specimens to observe temperature changes. For the metal specimen, this would require a slip-ring arrangement. With thermocouples, thermal equilibrium could be

observed, and the role of friction heat in the investigation studied.

3. The metal specimen has already been electrically insulated from the carbon specimen. This was done so that contact resistance might be studied. A Kelvin Bridge or similar resistance measuring circuit should be employed to record contact resistance changes with boundary film build-up. Observing contact resistance, friction, specimen temperature, and wear simultaneously should help in deciding what is happening between the surfaces to cause wear.

4. The metal specimens should be prepared by grinding them on the apparatus spindle. This can be done by removing the base plate from the micrometer bench and bolting it in place on a grinding machine. The spindle may be turned to achieve grinding by a belt connection as used on the apparatus.

BIBLIOGRAPHY

1. da Vinci, Leonardo, Notebooks, ed. and translated by Edward MacCurdy, Johnthan Cape, London, England, 1938.

2. Amentons, Histoire de 1'Academic Royal des Sciences Avic les Memories de Mathematique et de Physique, 1699.

3. Coulomb, C. A., Memories de Mathematique et de Physique de 1'Academic Royale des Sciences, 1785.

4. Bowden, F. P. and Tabor, D., Friction and Lubrication, Aberdeen University Press, London, England, 1956.

5. Burwell, "Survey of Possible Wear Mechanisms," Wear, Vol. I, No. 2, p. 155, October, 1956.

6. Holm, R., Electric Contacts Handbook, Gerber, Stockholm, Sweden, p. 214, 1946

7. Burwell, J. T. and Strang, C. D., "On the Empirical Law of Adhesive Wear," Journal of Applied Physics, Vol. 23, p. 18, 1952.

8. Archard, J. F., "Contact and Rubbing of Flat Surfaces," Journal of Applied Physics, Vol. 24, p. 981, 1953.

9. Dorinson and Broman, "Contact Stress and Load as Parameters in Metallic Wear," Wear, No. 2, Vol. 4, p. 93, March/April, 1961.

10. Halling, "A Crossed-Cylinder Wear Machine and Its Use in the Study of Severe Wear of Brass on Mild Stell," Wear, No. 1, Vol. 4, p. 22, January/February, 1961.

11. Lyddon and Hurden, "Some Mechanical Engineering Applications of Carbon," Industrial Carbon and Graphite, Society of Chemical Industry, London, 1957.

12. Millet, "Carbone et Contact Glessant," Industrial Carbon and Graphite, Society of Chemical Industry, London, 1957.

13. Milne, Scott, and Mac Donald, "Some Studies of Scuffing with a Crossed Cylinder Wear Machine," Proceedings of the Conference on Lubrication and Wear, The Institution of Mechanical Engineers, London, England, October, 1957.

APPENDIX I

METHOD OF CALCULATIONS

I Wear Volume:

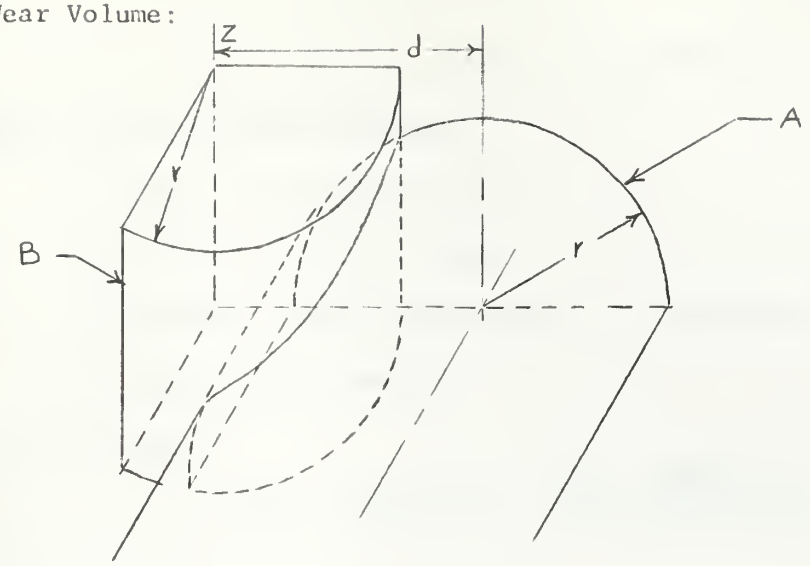

Figure 32

Two methods of calculating the intersected volume were used:

1. An equation was formed and solved by the author on the INTERCOM 1000 computer at NEES, Annapolis, Maryland.

2. A series solution derived by Halling was applied as a check on the computer solution.[10]

Equation for the computer solution. (See figure 32)

1. For circular cross sections of B, independent of z:

$$x^2 + y^2 = r^2. \tag{2}$$

2. For circular cross sections of A, independent of y:

$$z^2 + (x-d)^2 = r^2. \tag{3}$$

3. Elemental Volume: $dV = yz\,dx,$

but from (2) and (3): $y = (r^2 - x^2)^{1/2},$

$$z = [r^2 - (x-d)^2]^{1/2}.$$

4. Volume:

$$V = 4\int_{d-r}^{r}\left[r^2-(x-d)^2\right]^{\frac{1}{2}}(r^2-x^2)^{\frac{1}{2}}dx \tag{4}$$

Equation (4) was solved using $\Delta x = .000010$ and $\Delta d = .000100$.

Equation for the series solution.

a = radii of the hard metal

b = radii of the soft metal

d = depth of wear (assumed small in relation to a and b)

$2c$ = minor wear diameter

It is true that:

$$V = \pi\sqrt{ab}\,d^3 - \frac{\pi}{8}\sqrt{a+b}\,d^3 - \cdots, \tag{5}$$

$$C = \sqrt{2bd}\left(1-\frac{d}{4b}\right), \tag{6}$$

therefore;

$$V = \frac{\pi}{4}\sqrt{\frac{a}{b^3}}\,c^4 + \frac{\pi\sqrt{ab}}{8b^4}\left(1-\frac{a+b}{8a}\right)c^6\cdots,$$

or approximately,

$$V = \frac{\pi}{4}\sqrt{\frac{a}{b^3}}\,c^4$$

For this investigation, $a = b =$ .75",

so that,

$$V = 1.045\,c^4 \tag{7}$$

Comparison of Computer and Series Solutions.

(a) Depth of wear ----.0002"

$V = .0931 \times 10^{-6}/in^3$ ---computer

$V = .0936 \times 10^{-6}/in^3$ ---- series

(b) Depth of wear----.0016"

$V = 6.0255 \times 10^{-6}$ in^3 --- computer

$V = 6.0066 \times 10^{-6}$ in^3--- series

II Projected Contact Area:

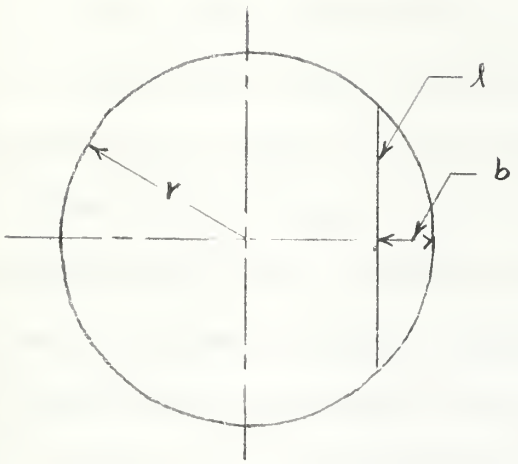

r = specimens diameter

b = depth of wear

ℓ = diameter of scar

Figure 33

It is true that:

$$\ell^2 = 4(2br - b^2) \tag{8}$$

but r = .75", so that:

$$\ell^2 = 6b - 4b^2. \tag{9}$$

The wear scar is nearly a circle for small depths of wear (figures) so that the area may be closely approximated from:

$$A = \frac{\pi \ell^2}{4}. \tag{10}$$

Figure 34 is a plot of volume and projected contact area vs. depth of wear. The actual curves used to reduce the data were plotted to a much larger scale.

III Test Runs:

Constant Load.

The runs were conducted as outlined in the Procedure Section. On

completion of the run, the wear scar diameter was determined by making two measurements, at right angles to each other with a microscope. The two measurements were averaged. With the diameter known, it was then possible to determine the depth of wear from previously prepared curves, such as figure 34. Now, using the run sensitivity (divisions of chart paper per inch of wear depth), and the known wear scar depth, the origin of the run was easily determined on the chart paper. Usually this origin could be determined, within a few divisions, by the trace appearance alone. Specimen run-out, however, causes some displacement of the recorder pen. The displacement is constant due to the high test speed and response characteristics of the instruments; the depth of wear is superimposed on the constant signal. By going through the above procedure, no error was introduced into the calculations due to using the wrong origin. With the known origin, it was simply a matter of picking off the number of divisions displaced at desired times, and applying the sensitivity to arrive at the wear depth. The volume was then taken from curves similar to figure 34.

EXAMPLE: (Data is taken from the 4 lb. load test for DSQ metal--CC carbon combination)

Final Wear Spot Diameter:

6.1401	5.9554
-5.9933	-5.8088
.1468 cm.	.1466 cm.

Average wear spot diameter = .1467 cm. or .0576 in.

Run Sensitivity:

48 div./.001" or .0208 x 10^{-4} in./div.

Entering figure 34 with .0576 in. diameter, the corresponding depth of 5.57 x 10^{-4} in. is found. Applying the run sensitivity, this corresponds to 26.8 divisions on the chart paper. Since the termination of the

recorded trace is the end of the wear run, the origin of the run may easily be established on the trace by counting off 26.8 divisions from the terminating point.

Adjusted Constant Pressure

The runs were conducted as outlined in the Procedure Section. As a run progressed, the wear spot diameter was measured at intervals so that the load could be adjusted. To accomplish this, the area was determined from the diameter and the relation Pressure = $\frac{\text{load}}{\text{area}}$ applied. The volume and area were taken from curves such as figure 34.

Coefficients of Friction

Weights of .1 lb. were suspended from the friction beam, and the number of divisions displaced by the recorder pen noted. The displacement was 13 divisions in each case. The relation

$$\text{Coefficient of Friction} = \frac{\text{Friction Force}}{\text{Normal Load}}$$

was used for calculations. The Friction Force was obtained from the trace and the Normal Load was known.

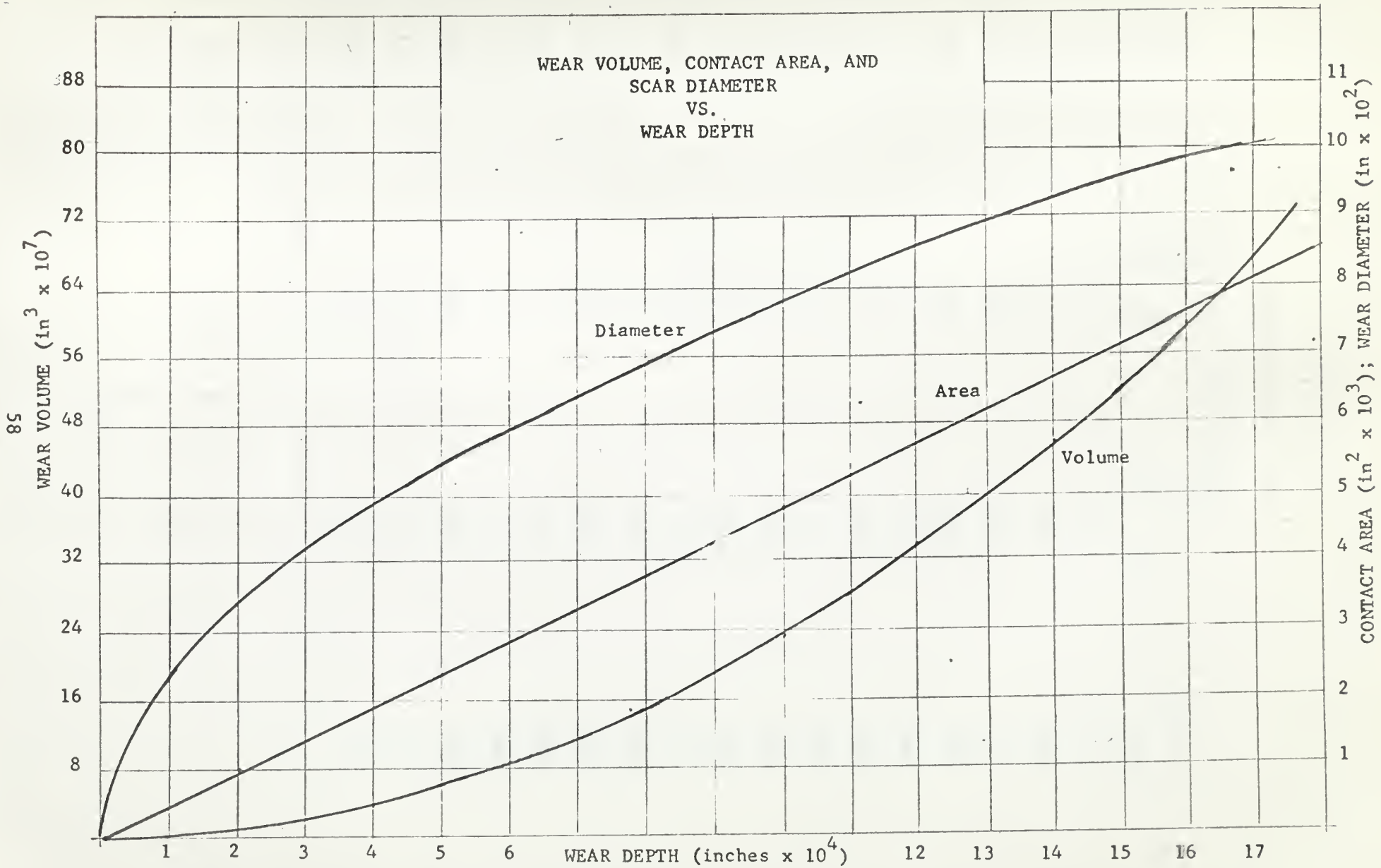
WEAR VOLUME, CONTACT AREA, AND
SCAR DIAMETER
VS.
WEAR DEPTH
Diameter
Area
Volume
WEAR VOLUME (in^3 x 10^7)
CONTACT AREA (in^2 x 10^3); WEAR DIAMETER (in x 10^2)
WEAR DEPTH (inches x 10^4)
85
88
80
72
64
56
48
40
32
24
16
8
11
10
9
8
7
6
5
4
3
2
1
1
2
3
4
5
6
12
13
14
15
16
17

FIGURE 34

APPENDIX II

CONSTANT LOAD TESTS

Load 2 lb.; Spd. 3000 RPM

Time (min)	Depth (in x 10^4)	Volume (in^3 x 10^8)	Pressure (psi)
0.25	3.45	27.7	1230
0.50	3.67	31.3	1160
0.75	3.74	32.3	1135
1.00	3.89	35.0	1095
1.50	4.10	39.0	1040
2.00	4.25	42.0	1000
2.50	4.35	44.0	980
3.00	4.43	45.5	965
4.00	4.52	47.2	945
5.00	4.65	50.0	915
6.00	4.69	51.1	910
7.00	4.74	52.2	900
8.00	4.76	52.5	895
9.00	4.78	53.2	890
10.00	4.80	53.8	887
11.00	4.84	54.8	880
12.00	4.91	56.2	867

APPENDIX II

CONSTANT LOAD TESTS

Load 3 lb.; Spd. 3000 RPM

Time (min)	Depth (in x 10^4)	Volume (in^3 x 10^8)	Pressure (psi)
0.25	3.24	24.7	1975
0.50	3.66	31.0	1750
0.75	3.74	32.5	1710
1.0	3.95	36.0	1620
1.50	4.12	39.2	1550
2.0	4.22	41.2	1520
2.50	4.35	44.0	1470
3.0	4.38	44.8	1460
4.0	4.47	46.5	1430
5.0	4.60	44.0	1390
6.0	4.67	50.5	1365
7.0	4.83	54.3	1325
8.0	4.85	55.0	1320
9.0	4.97	58.0	1285
10.0	5.02	59.0	1275
11.0	5.06	60.2	1260
12.0	5.15	62.5	1240

APPENDIX II

CONSTANT LOAD TESTS

Load 4 lb.; Spd 3000 RPM

Time (min)	Depth (in x 10^4)	Volume (in^3 x 10^8)	Pressure (psi)
0.25	2.39	13.2	3570
0.50	2.87	14.2	2970
0.75	3.22	24.2	2650
1.0	3.54	29.1	2410
1.50	3.82	33.7	2230
2.0	4.10	39.0	2080
2.50	4.33	43.0	1970
3.0	4.51	47.1	1890
4.0	4.70	51.2	1810
5.0	4.85	55.0	1760
6.0	5.00	58.8	1705
7.0	5.14	62.3	1660
8.0	5.30	66.2	1610
9.0	5.39	68.8	1580
10.0	5.47	70.5	1560
11.0	5.53	72.0	1540
12.0	5.57	73.2	1530

APPENDIX II

CONSTANT LOAD TESTS

Load 5 lb; Spd 3000 RPM

Time (min)	Depth (in x 10^4)	Volume (in^3 x 10^8)	Pressure (psi)
0.25	2.23	11.5	4770
0.50	2.81	18.2	3790
0.75	3.16	23.4	3370
1.0	3.45	27.8	3090
1.50	3.89	35.0	2740
2.0	4.20	41.0	2540
2.50	4.43	45.5	2410
3.0	4.57	48.5	2320
4.0	4.76	52.7	2240
5.0	4.44	57.3	2150
6.0	5.14	62.3	2080
7.0	5.31	65.2	2010
8.0	5.41	69.0	1970
9.0	5.47	70.6	1445
10.0	5.56	72.7	1915
11.0	5.73	77.0	1860
12.0	5.80	79.0	1835

APPENDIX II

ADJUSTED CONSTANT PRESSURE TESTS

500 psi Speed-3000 RPM

Time (m-s)	Dia. (in)	Area ($in^2 \times 10^3$)	Depth ($in^3 \times 10^4$)	Vol. ($in^3 \times 10^8$)	Reg.Ld. (lb)	Ad,LD (lb)	Error (%)
0	.0364	1.05	2.25	11.8	.525	.50	5.0
-15	.0374	1.12	2.35	13.0	.56	.60	7.0
-30	.0404	1.30	2.77	17.8	.65	.60	8.0
-45	.0424	1.42	3.00	21.0	.71	.70	1.4
1-00	.0424	1.42	3.00	21.0	.71	.70	1.4
1-15	.0424	1.42	3.00	21.0	.71	.70	1.4
2-00	.0434	1.50	3.20	24.0	.75	.80	6.4
3-00	.0443	1.57	3.31	25.6	.785	.80	2.0
5-00	.0443	1.57	3.31	25.6	.785	.80	2.0
7-00	.0454	1.63	3.45	27.8	.81	.80	2.0
9-00	.0454	1.63	3.45	27.8	.81	.80	2.0
11-00	.0468	1.71	3.65	31.0	.0855	.90	5.0
13-00	.0472	1.78	3.75	32.5	.89	.90	5.1
15-00	.0472	1.78	3.75	32.5	.89	.90	5.1
17-00	.0480	1.83	3.90	35.0	.915	.90	1.4

APPENDIX II

ADJUSTED CONSTANT PRESSURE TESTS

8 00 psi — Speed-3000 RPM

Time (m-s)	Dia. (in)	Area ($in \times 10^{3}$)	Depth ($in \times 10^{4}$)	Vol ($in^{3} \times 10^{8}$)	Reg.Ld. (lb)	Ad.Ld. (lb)	Error (%)
0	.0246	.7	1.5	5	.56	.60	7.5
-15	.0354	1.0	2.1	10.2	.80	.80	0.0
-30	.0374	1.12	2.4	13.2	.90	1.00	11.2
-45	.0384	1.20	2.5	14.5	.96	1.00	4.4
1-00	.0414	1.40	3.0	21.0	1.12	1.20	7.5
1-15	.0432	1.50	3.2	23.2	1.20	1.20	0.0
2-30	.0444	1.60	3.4	27.0	1.28	1.20	6.3
3-00	.0454	1.64	3.5	28.5	1.31	1.30	0.9
4-00	.0473	1.75	3.7	31.5	1.40	1.40	0.0
5-00	.0493	1.90	4.0	38.0	1.52	1.50	1.5
6-00	.0493	1.90	4.0	38.0	1.52	1.50	1.5
7-00	.0493	1.90	4.0	38.0	1.52	1.50	1.5
8-00	.0513	2.08	4.4	44	1.66	1.70	2.1
10-00	.0523	2.18	4.6	49	1.75	1.80	3.3
14-00	.0532	2.21	4.7	51	1.77	1.80	1.8
16-00	.0550	2.40	5.1	61	1.92	1.90	1.2
22-00	.0555	2.45	5.3	65	-	-	-

APPENDIX II

ADJUSTED CONSTANT PRESSURE TESTS

1000 psi — Speed-3000 RPM

Time m-s	Dia. (in)	Area ($in \times 10^{3}$)	Depth ($in \times 10^{4}$)	Vol. ($in^{3} \times 10^{8}$)	Reg.Ld. (lb)	AdjLd. (lb)	Error (%)
0	.0374	1.10	2.35	12.9	1.10	1.10	0.0
0-15	.0414	1.39	2.90	19.8	1.39	1.40	0.1
0-30	.0434	1.50	3.16	23.3	1.50	1.50	0.0
0-45	.0513	2.10	4.40	44.0	2.10	2.10	0.0
1-00	.0532	2.21	4.72	51.8	2.21	2.20	0.1
1-15	.0542	2.31	4.96	57.8	2.31	2.30	0.1
1-45	.0552	2.41	5.15	62.0	2.41	2.40	0.1
2-45	.0552	2.41	5.15	62.0	2.41	2.40	0.1
3-45	.0581	2.70	5.71	76.3	2.70	2.70	0.0
4-45	.0591	2.79	5.90	81.6	2.79	2.80	0.1
6-45	.0620	3.00	6.40	93	3.00	3.00	0.0
8-45	.0640	3.20	6.85	105	3.20	3.20	0.0
10-45	.066	3.38	7.20	120	3.38	3.40	0.1
12-45	.067	3.50	7.45	130	3.50	3.50	0.0
14-45	.068	3.60	7.70	140	-	-	-

APPENDIX II

ADJUSTED CONSTANT PRESSURE TESTS

1830 psi — Speed-3000 RPM

Time m-s	Dia. (in)	Area ($in \times 10^{3}$)	Depth ($in \times 10^{4}$)	Vol. ($in^{3} \times 10^{8}$)	Reg. ld (lb)	Adj. ld. (lb)	Error (%)
0	.0407	1.31	2.80	18.0	2.40	2.40	0.0
0-15	.0435	1.50	3.15	23.3	2.79	2.80	2.2
0-30	.0428	1.80	3.82	33.6	3.30	3.20	2.7
0-45	.0493	1.91	4.10	34.0	3.50	3.60	3.0
1-00	.0513	2.10	4.42	45.2	3.84	3.80	1.1
1-20	.0532	2.21	4.78	51.5	4.04	4.00	1 1
1-45	.0532	2.21	4.78	51.5	4.04	4.00	1.1
2-30	.0570	2.59	5.50	65.0	4.74	4.80	1.1
3-30	.0590	2.76	5.90	81.7	5.05	5.00	1.1
4-00	.0590	2.76	5.90	81.7	5.05	5.00	1.1
5-00	.064	3.20	6.90	93.0	5.85	5.80	1.1
7-00	.0649	3.28	7.00	112	6.00	6.00	0.0
9-00	.0672	3.51	7.52	132	6.42	6.40	0.5
12-00	.0692	3.75	8.00	150	6.86	6.80	1.1

APPENDIX II

VARYING SPEED TEST DATA

		Speed-600 RPM	
Time (min)	Depth (in x 10^4)	Volume (in^3 x 10^8)	Distance (ft)
0.25	.62	1.2	59
0.50	.77	1.8	118
0.75	.83	1.9	177
1.0	.92	2.0	236
1.5	1.06	2.7	353
2.0	1.19	3.2	471
2.50	1.40	4.4	590
3.0	1.60	5.8	706
4.0	2.04	9.8	941
5.0	2.43	18.5	1179
6.0	2.81	18.2	1415
7.0	3.15	23.2	1650
8.0	3.39	25.2	1885
9.0	3.64	30.8	2120
10.0	3.84	34.0	2355
11.0	4.04	38.0	2590
12.0	4.25	42.0	2825

APPENDIX II

VARYING SPEED TEST DATA

Speed-1020 RPM			
Time (min)	Depth ($in \times 10^4$)	Volume ($in^3 \times 10^8$)	Distance (ft)
0.25	1.66	6.2	100
0.50	1.94	8.8	200
0.75	2.08	10.1	300
1.0	2.14	10.8	400
1.50	2.37	13.1	600
2.0	2.62	15.7	800
2.50	2.83	18.5	1000
3.0	3.00	21.0	1200
4.0	3.36	26.3	1600
5.0	3.60	30.0	2000
6.0	3.80	33.5	2400
7.0	4.05	38.0	2800
8.0	4.24	41.8	3200
9.0	4.41	45.0	3600
10.0	4.55	48.0	4000
11.0	4.72	51.3	4400
12.0	4.83	54.2	4800

APPENDIX II

VARYING SPEED TEST DATA

Speed-1980 RPM

Time (min)	Depth ($in \times 10^4$)	Volume ($in^3 \times 10^8$)	Distance (ft)
0.25	1.29	3.8	194
0.50	1.56	5.4	387
0.75	1.69	6.5	582
1.0	1.85	8.0	775
1.50	2.10	10.2	1160
2.0	2.33	12.5	1550
2.50	2.50	14.3	1935
3.0	2.66	16.2	2320
4.0	2.79	18.0	3100
5.0	2.82	18.2	3870
6.0	3.04	21.7	4150
7.0	3.16	23.2	5430
8.0	3.16	23.2	6200
9.0	3.18	23.8	6960
10.0	3.18	23.8	7750
11.0	3.21	24.1	8530
12.0	3.4	24.1	9300

APPENDIX II

VARYING SPEED TEST DATA

Speed-3000 RPM

Time (min)	Depth (in x 10^4)	Volume (in^3 x 10^8)	Distance (ft)
0.25	1.17	2.54	294
0.50	1.39	4.4	587
0.75	1.45	4.7	881
1.0	1.58	5.7	1175
1.50	1.72	6.7	1760
2.0	1.84	7.9	2350
2.50	2.02	9.4	2940
3.0	2.08	10.1	3530
4.0	2.28	12.0	4700
5.0	2.45	13.9	5870
6.0	2.65	16.1	7050
7.0	2.80	18.1	8230
8.0	2.91	19.5	9400
9.0	3.00	21.0	10570
10.0	3.08	22.3	11750